INVESTIGATION OF THE EFFECTS OF ECO-FRIENDLY NANOFLUIDS THROUGH MINIMUM QUANTITY LUBRICATION IN GRINDING METAL MATRIX COMPOSITE

By

Md. Ashab Shakur

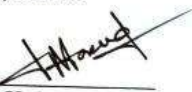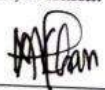A Thesis
Submitted to the
Department of Industrial & Production Engineering
in Partial Fulfilment of the
Requirements for the Degree
of
M.Sc. in Industrial and Production Engineering

**DEPARTMENT OF INDUSTRIAL & PRODUCTION ENGINEERING
BANGLADESHUNIVERSITY OF ENGINEERING & TECHNOLOGY
DHAKA, BANGLADESH**

April 2023

The thesis titled "**Investigation of the Effects of Eco-friendly Nanofluids through Minimum Quantity Lubrication in Grinding Metal Matrix Composite**"submitted by **Md. Ashab Shakur**, Student No. 0419082012, Session - April 2019, has been accepted as satisfactory in partial fulfillment of the requirement for the degree of Master in Industrial and Production Engineering on April 29, 2023.

BOARD OF EXAMINERS

1. Dr. Nikhil Ranjan Dhar
   Professor
   Department of Industrial & Production Engineering
   BUET, Dhaka.

   Chairman

2. Dr. Ferdous Sarwar
   Professor & Head
   Department of Industrial & Production Engineering
   BUET, Dhaka

   Member
   (Ex-officio)

3. Dr. A. K. M Masud
   Professor
   Department of Industrial & Production Engineering
   BUET, Dhaka.

   Member

4. Dr. Prianka Binte Zaman
   Associate Professor
   Department of Industrial & Production Engineering
   BUET, Dhaka.

   Member

5. Dr. Mohammad Muhshin Aziz Khan
   Professor
   Department of Industrial & Production Engineering
   Shahjalal University of Science and Technology
   Sylhet

   Member
   (External)

Declaration

It is hereby declared that this thesis or any part of it has not been submitted elsewhere for the award of any degree or diploma.

মো: আসহাব শাকুর
_____
Md. Ashab Shakur

This work is dedicated
to my 'loving parents'

Md. Aslam Mia
And
Shamim Ara Begum

Table of Contents

List of Figures

List of Tables

List of Symbols

D	**:**	Diameter of the tool (mm)
d	**:**	Infeed (μm)
G	**:**	Grinding Ratio
T	**:**	Cutting temperature (^{0}C)
R	**:**	Surface roughness (μm)
Al/SiC-MMC	**:**	SiC reinforced Al based MMC
ANN	**:**	Artificial neural network
DoE	**:**	Design of Experiments
RSM	**:**	Response surface methodology
CBN	**:**	Cubic boron nitride
CDA	**:**	Composite desirability approach
CCD	**:**	Central composite design
DF	**:**	Degree of Freedom
DI	**:**	Deionized
APE	**:**	Absolute percentage error
MAPE	**:**	Mean absolute percentage error
NF	**:**	Nanofluid
NP	**:**	Nanoparticle
N_s	**:**	Spindle speed (RPM)
ρ	**:**	Density (Kg/m^{3})
MQL	**:**	Minimum quantity lubrication
MRR	**:**	Material removal rate
MMC	**:**	Metal matrix composite
nMQL	**:**	Nanofluid minimum quantity lubrication
SEM	**:**	Scanning electron microscope
SiC	**:**	Silicon carbide
WW	**:**	Wheel Wear (μm^{3})

Acknowledgements

Abstract

The unique physical features and reliability of advanced composite materials have attracted interest in recent years. Aluminum MMCs reinforced with SiC particles (Al/SiC-MMC) exhibit a yield strength increase of up to 20%, a greater modulus of elasticity, a lower coefficient of thermal expansion, and are more resistant to wear than the corresponding unreinforced matrix alloy systems. Despite having many benifits, Al/SiC-MMC shows poor machinability. Process such as grinding is crucial for the material to obtain aquality finish and damage-free surfaces. But soft aluminum alloys have poor grindability due to chip adherence, thereby clogging the wheel. Periodic dressing is required to avoid the aforementioned issues, which makes the grinding process inefficient. An effective cooling approach thus needs to be used with optimal process parameters that will enhance the grindability of the Al/SiC-MMC. The present work investigates the effects of the application of ecofriendly ZnO-deionized water nanofluid on the grindability of Al/SiC-MMC by CBN grinding wheel in respect of chip morphology, grinding temperature, surface roughness, wheel wear, and grinding ratio. A suitable MQL set-up has been designed and fabricated to deliver variable MQL flow rate continuously at the critical zones during surface grinding of the workpiece. In order to prepare the nanofluids, 0.5% volume of ZnO & Sodium dodecyl sulphate (SDS) surfactant are dispersed in the deionized water performing ultra-sonication & magnetic stirring for thirty minutes each. Experiments are designed using central composite design and empirical models are developed to predict grinding temperature, wheel wear, and surface roughness through RSM for flood cooling & MQL. Based on the experimental data, empirical model for predicting surface roughness has been developed using artificial neural network. Application of the produced nanofluids through MQL significantly reduces the cutting temperature, surface roughness, & wheel wear of the material and improves the grinding ratio compared to conventional flood cooling method. Significant reduction inclogging of the workpiece material into the CBN grinding wheel is observed for the MQL compared to dry grinding and flood cooling. Spindle speed 3000 rpm, infeed 10 μm, and environment nMQL have been selected using RSM based composite desirability approach to be the desired optimal combination for enhancing the grindability of Al/SiC-MMC.

Chapter-1

Introduction

1.1   Introduction

Composite materials encompassing metal matrix composites (MMC), ceramic matrix composites, and polymer matrix composites are increasingly being utilized in aerospace applications (Klocke et al., 2015). MMCs are broadly used in the military, astronautic, and automobile industries, capitalizing on the materials' high specific properties. Among the MMC family, Al is preferred as a matrix because of its excellent engineering properties, easy producibility, and low-density capabilities (Nas & Gökkaya, 2017). Inspite of having many benefits, full implementation of MMCs is costly, partially because of the material's poor machinability. Many machining processes often result in cracking, splintering, and pullingout of reinforcement objects. Sub-surface damage might occur from conventional and unconventional processes, such as turning, drilling, milling, electrical discharge machining, and laser machining (Zhong & Hung, 2002). Besides, MMCs reinforced with SiC have lesser machinability than those reinforced with Al_2O_3 (Hung et al., 1997). Process such as grinding is crucial for the application of these materialsto obtain a smooth surface finish and damage-free surfaces (Zhong & Hung, 2002). Besides, While grinding Aluminium metal matrix composite with CBN wheels, wheel loading with soft aluminium matrix was observed which in turn, blocked wheel grains. Blocking of wheel grains results in increased friction, thereby increasing grinding forces (Hung et al., 1997). It also requires frequent redressing of the wheel and thus reduces the efficiency of the process. An appropriate method should be adopted that will increase the grindability of Al/SiC-MMC with CBN grinding wheels.

Grinding is a machining process that uses tools with a large number of randomly oriented abrasive particles, with mostly negative rake angles, retained by a bonding material (Aurich & Effgen, 2014). Grinding is traditionally used as a finishing operation as

it is capable of obtaining high dimensional accuracy and surface finish by removing a small amount of material (Nandakumar & Rajmohan, 2018). Dimensional tolerances of less than 1 μm and surface roughness as fine as .025 μm can be achieved with this process (Kalpakjian & Schmid, 2013). Despite the superior surface quality achieved by this process, it has certain features that can ruin the desired surface quality if not properly addressed. Unlike conventional machining processes such as turning, drilling, and milling operations, grinding is a high cutting-speed application that requires higher specific energy values, thereby resulting in high temperature generation at chip-tool interface, usually over 600°C. The high surface temperatures cause rapid tool wear and several possible damages to the work, such as surface burning, cracking, softening of the work surface, poor surface integrity, and generating residual stresses (Aurich et al., 2008; Groover, 2020). Hence, a method should be adopted that will carry the heat generated away from the grinding zone. The application of conventional cutting fluids to the grinding area has been adopted as a popular way to mitigate the problem. However, conventional cutting fluids possess remarkable disadvantages that limit their applications in machining processes. Several uses of these fluids may lead to chemical changes in their properties. In addition, using these fluids several times may lead to oil contamination. Oil contamination and chemical changes can reduce the performance of the cutting fluid and may have adverse impacts on the environment (Hosseini Tazehkandi et al., 2015). Consequently, it has become a crucial task for the researchers to search for suitable cutting fluid that can address the temperature related problem and at the same time ensure environment friendliness as well. Nanofluids have been receiving great attention from researchers in recent years because they exhibit superior thermal properties compared to their host fluids (Choi, 1995). These nanofluids can provide better thermal conductivity along with better lubrication capabilities (Das et al., 2007). In order to be utilized effectively in grinding operations, both their thermal and lubrication properties should remain capable at elevated temperatures. Another issue that needs to be kept in mind while choosing nanoparticles is that they should have antibacterial, antimicrobial, and non-toxic properties to be environment-friendly and sustainable.

In an attempt to apply cutting fluid to the grinding zone, the flooding method are most commonly practiced. However, the effectiveness of this method in reaching the grinding zone has been questioned by many researchers as only 4 to 30% of the applied

fluid could reach the grinding area because of an air barrier around the grinding wheel (Mandal et al., 2012). So, the selection of an appropriate mode of cutting fluid is also vital in reducing grinding zone temperature and thereby getting a product with desired surface quality.

This chapter presents necessary background information related to this research work. Besides, some topics are discussed thoroughly in this chapter, such as the selection of grinding wheel, selection of cutting fluid, and high temperature generation in grinding. Also, this chapter includes literature review, objectives of the study, scope of the study, and organization of the thesis.

1.2   Literature review

1.2.1 Selection of grinding wheel

In grinding, abrasives are bonded together into a wheel with the help of bonding material. The bonding material also establishes the shape and structure of the wheel (Black & Kohser, 2012; Groover, 2020). Choosing the appropriate abrasive material for grinding depends on the work material. General properties of abrasive particles used in grinding wheels include high hardness, wear resistance, toughness, and friability. The grinding wheel has self-sharpening ability. Therefore, abrasive particles either fracture to create fresh cutting edges or are pulled out of the surface of the wheel to expose new grains as these become dull as a result of wheel wear. Friability refers to the characteristic of the abrasive material to fracture while the grain's cutting edge becomes dull, thus exposing a new sharp edge (Groover, 2020). Greater friability of grains is better for low grinding forces (Rowe, 2013). Some abrasives are found in nature while some are artificially made. Sandstone, emery, corundum (natural Al_2O_3), sand, quartz, garnet, and diamond are some examples of natural abrasives. As they contain impurities and have non-uniform properties in their natural state, their performance as abrasive is inconsistent and unreliable. Hence, synthetic abrasives have been made for many years, such as aluminum oxide, silicon carbide, cubic boron nitride, and diamond (also known as synthetic or industrial diamond). Diamond and cubic boron nitride are categorized as superabrasives since they are the two

3

hardest materials known (Kalpakjian & Schmid, 2013). Some recommendations on selecting abrasives based on work material are given below:

- **Aluminum oxide:** Carbon steels, alloy steels, and ferrous alloys.
- **Silicon carbide:** Nonferrous metals, cast irons, ceramics, glass, and marble. Ductile metals such as aluminum, brass as well as brittle materials such as some cast irons and certain ceramics. It is not effective for grinding steel because of the strong chemical affinity between the carbon in SiC and the iron in steel.
- **Cubic boron nitride:** It is used for high hardness (i.e. above 50 HRC) steels and cast irons, such as hardened tool steel; high temperature alloys such as aerospace alloys.
- **Diamond:** It has applications on hard, abrasive materials such as ceramics, carbides, and glass (Groover, 2020; Kalpakjian & Schmid, 2013)

As discussed before, extremely abrasive SiC can cause quick tool wear (Shanawaz et al., 2011). That's why the wheel that will be used for its grinding should possess significant wear resistance capability. CBN wheels possess greater wear resistance than conventional wheels. Besides, CBN wheel has a superior size holding capacity and a longer wheel redress life. When compared to typical aluminium oxide or silicon carbide wheels, CBN abrasives have a higher thermal conductivity, allowing for cooler grinding. This enables significantly faster removal rates while avoiding thermal damage or tensile residual stress. Though CBN wheels are significantly more expensive than conventional wheels, expenses associated with conventional grinding wheels may be more significant. These costs may include downtime associated with more frequent wheel changes, set-up costs, and more frequent redressing costs. Additionally, selected CBN grains are often smaller in size than traditional wheels used for the same grinding activity. This property enables the use of sharp CBN grains to create reduced surface roughness (Chen et al., 2002). A significant advantage of CBN is its low partition ratio, which allows for significant reductions in the temperatures encountered by the workpiece (Rowe et al., 1997). For all of these reasons, CBN wheels are chosen to be used in this study for grinding Al/SiC-MMC.

1.2.2 Chip formation in grinding

The study of grinding chips is very crucial in understanding the mechanism of chip formation. Tso (Tso, 1995) classified grinding chips into six categories: shear, melt, flow, rip, knife, and slice. The size of the chips generated during grinding may vary greatly because of the cutting edges' random position on the grinding wheel (Li et al., 2016). However, because small variations in the chip formation process can affect workpiece surface quality, workpiece precision, and grinding wheel life, chip creation is particularly crucial in machining. Additionally, unfavorable chip formation may result in worker accidents, a poor surface polish, and damage to the tool, workpiece, and machine equipment, all of which might increase expenses due to downtime, scrap production, and production delays (Jawahir et al., 1993). A deeper understanding of chip creation and the relationship between input and output parameters are all necessary to address these issues.

The slice type is large enough that it isvisible upon scrutiny. When the grinding wheel goes through heavy loading, slice type chips occur. Wheel loadingis the deposition of chips in the gap between the grains of a grinding wheel. It is responsible for shortening tool life, greater cutting force, the greater amount of power requirement, etc. When a wheel becomes loaded, it causesincreased cutting force. If the grinding force exceeds the bonding strength of the grinding wheel, the loaded chip thenfalls off, creating a slice type chip. This type of chip is less likely to occur while grinding with silicon carbide (GC) wheels due to the low loading of chips.The knife-type chip arises before the slice-type chip when the wheel is under slight loading, according to experimentalobservation. With its smaller loading area and superior workpiece surface, it is easier to find knife-type chips in placeswhere the slice-type chips are found.Ripping type chip occurs when the wheel is under heavy attritious wear with low loading situation. Because of thehigh grinding temperature caused by severe attritious wear, the workpiece surface seems a bit burnt under themicroscope, with some chips sticking to it.Shearing type chip is comparatively greater in both length and straightness than slice, knife, and ripping chips. Thischip is produced when there is less attritious wear on the grinding wheel. As a result of reduced attritious wear, thecutting edge of the grinding wheel remains sharper, and the workpiece surface is better. Furthermore, when thegrinding wheel's attritious wear increases, the length of the shearing type chip reduces. Flowing-type chips are common in the grinding

process when the Aluminum oxide (WA), GC, or cubic boron nitride (CBN) wheels have just finished truing and dressing. For this chip type, the cutting edge of the grinding wheel is thesharpest among the other chip kinds. However, in the situation of either incorrect grinding settings or no grinding fluid, an entirely distinct chip type, namelythe melting type, arises. Because a high quantity of grinding heat is created and passed into the chips, the chips are melted separately.The dullness of the grinding wheel allows for a variety of chips to form throughout the grinding process. As a result,the kind of chip obtained may be taken as an indication that the wheel becomes dull enough that it requires to bedressed for further usage. Hence, chip type may be used as a criterion for grinding wheel dressing and truing.

Chip formation mechanisms are essential concerns to regulate the wheel performance or surface roughness of the workas well as optimization of input parameters (Dai et al., 2015; Li et al., 2016). But understanding the chip formation mechanism by runningexperimental observations is very challenging due to the interactions between several abrasive grains and theworkpiece material simultaneously. Researchers have recently attempted to investigate chip formation mechanismsconsidering single-grain grinding wheels. It has been found that the mechanical characteristics of the workpiecematerial such as ductility, hardness, and yield strength largely determine the chip formation behavior (Dai et al., 2015; Tso, 1995). Becauseof the combined effect of strain hardening, strain-rate hardening, and thermal softening, both grinding speed andundeformed chip thickness have a significant impact on chip formation (Calamaz et al., 2008; Guo et al., 2004; Sima et al., 2010). The grains act as the cutting toolsin a grinding wheel, and their shape and orientation determine how much material is to be removed. Both the shapesand the orientations of the grains are randomly distributed which alter with wear. The quantity of material removal byindividual grains determines the grinding forces and grinding wheel wear. Sharp grains outperform dull, worn grains by a wide margin (Rowe, 2013).

| (a) | (b) |
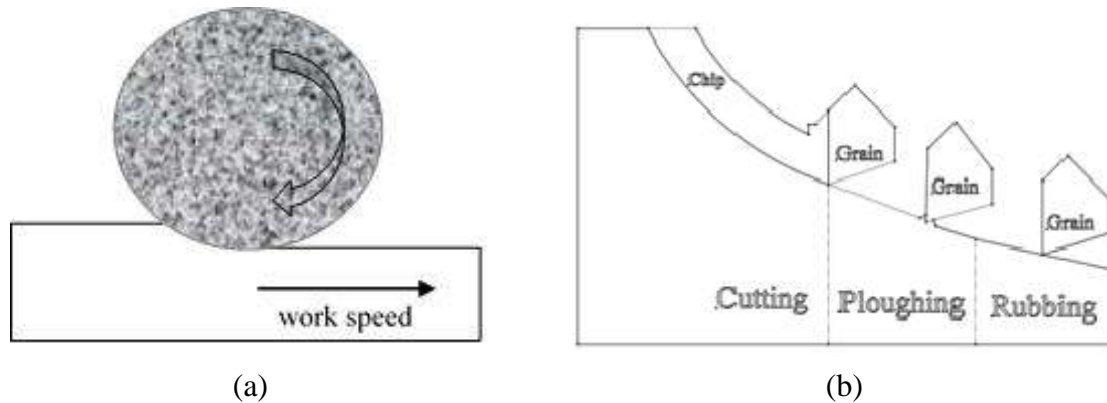
Fig. 1.1 (a) Material removal in up grinding (Rowe, 2013) (b) Material removal steps involved in grinding (Rowe et al., 2003)

Chip formation in grinding can be explained through the modified slip-line field method. This approach is beneficial since it takes into account the effects of friction and plastic deformation on chip creation. According to this model, metal removal in grinding is a three-step process; rubbing, ploughing, and cutting, consecutively, as shown in Fig. 1.1. At the beginning of the first stage, grain contacts the work surface but only rubbing friction occurs between them. As a result, the initial step consists entirely of elastic deformation of the workpiece. Energy is consumed without any material removal and this energy is converted into heat that heats the work, thereby decreasing the yield stress of the material (Groover, 2020; Lortz, 1979).

The normal force, tangential force, and frictional force rise progressively while the grain traverses the surface. The cutting edge penetrates the work when the normal stress surpasses the metal's yield stress. During the ploughing phase, work surfaces are distorted but no material is removed since the grain does not penetrate far enough into the work to produce cutting. A "dead zone" has been created between the cutting edge and the workpiece during the ploughing stage where no plastic flow takes place. This is because the grain shape is considered to be spherical in this model. Therefore, there remains no gap between the work and the grain to ensure the flow of materials but upwards and to the sides. The contacting region in front of the edge will compress the material, creating a distorted surface due to additional material flow. Hence, this stage creates a depression on the work surfaceas well as piled-up surfaces in front and alongside the depression (Lortz, 1979; Rowe et al., 2003). A shift from ploughing to chip generation happens if the deformed surface ahead of the cutting edge is piled up to such a level that it comes in the way of the cutting edge. The cutting edge's penetration into the plastic zone leads to an

increase in stress until the workpiece material's maximum shear strain energy is attained. The borderlines of the dead zone, known as slip lines, show discontinuities in tangential velocity. In actuality, it is predicted that plastic deformation will occur along these lines. Because the maximum shear stress lines are identical to the slip lines for isotopic materials, a narrow zone of metal deformation must develop at these lines, leading to local hardening. Thus, these lines denote places of intense plastic deformation (Lortz, 1979).

Because it dictates the geometry of the primary deformation, the shear angle has a significant impact on anticipating the machining process. Although Ernst and Merchant model is built on the assumption that the direction of shear corresponds with the direction of highest shearing stress, the shear angle solution from the model has been frequently employed in the past. The Ernst and Merchant model is expressed as follows(Hyung Wook Park et al., 2008):

$$\varphi = \frac{\pi}{4} - \frac{1}{2}(\beta - \alpha) = \tan^{-1}(\frac{r\cos\alpha}{1 - r\sin\alpha}) \quad \text{.. (1.1)}$$

where β is friction angle, r is chip thickness ratio, and α is rake angle. Chip thickness ratio can be calculated from the equations below:

$$r = \frac{t_1}{t_2} = \frac{\sin\varphi}{\cos(\varphi - \alpha)} = \frac{l_2}{l_1} \quad \text{.. (1.2)}$$

where t_1 = chip thickness before cutting

t_2 = chip thickness after cutting

l_1 = chip length before cutting

l_2 = chip length after cutting

t_2 is hard to measure due to the surface roughness of the outer chip surface. Hence, r can be calculated from the l_1 and l_2 values. Shear angle $\varphi_1, \varphi_2, \varphi_3$ is depicted in figures for flow, shear, and knife chips accordingly where $\varphi_3 < \varphi_2 < \varphi_1$. Based on the cutting circumstances, the shear angle has a broad range of possible values (Merchant, 2004). The range of shear angles considered by kocaefe (Kocaefe, 2017) lies between $10\overset{\circ}{\circ}$ to $40\overset{\circ}{\circ}$. When the shear angle increases, the shear area decreases as well as cutting force (Daymi et al., 2009).

(a) Flowing chip formation   (b) Shearing chip formation

(c) Knife type chip formation
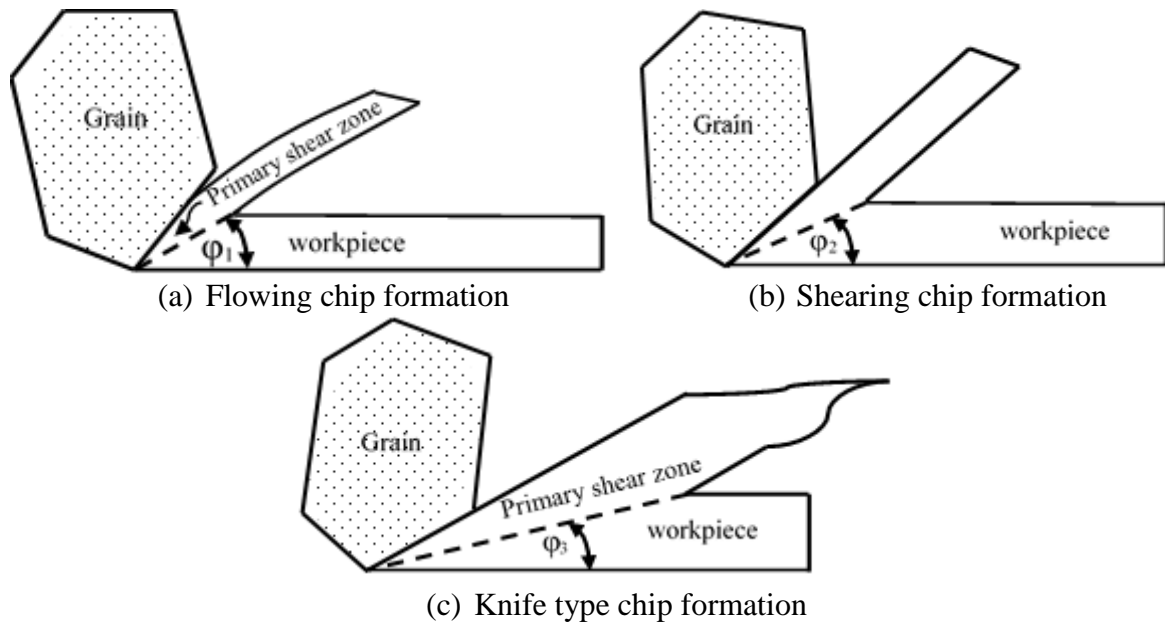
Fig. 1.2 Different chip formation (Li et al., 2016)

When the shear angle is small, shearing action deforms and piles up the material in front of the grain, which is more relevant to high compressive stress, resulting in the creation of a shear chip. There are several markings on the chip surface because the material stacked up at the front of the grain partly flows under the cutting edge. This type of chip has a high specific grinding force and raises the temperature of the grinding process (Li et al., 2016).

1.2.3 High temperature generation in grinding

Specific energy provides an essential measure of how much power is required to remove a unit volume of metal during machining. Tool sharpness, size effect, rake angle, cutting speed, and cutting fluid influence specific energy values. Worn tools require more power to perform cutting than sharp tools. This is reflected by high specific energy values for worn tools. With the increase of rake angle or cutting speed, or with the addition of cutting fluid, specific energy values reduce slightly. The size effect, negative rake angles, and ineffective grain actions altogether make the grinding process inefficient with respect to specific energy values. However, with a reduction of chip thickness before cut, specific energy requirement increases. This relationship is known as the size effect. As grinding produces far smaller chips compared to most other machining processes, it consumes very high specific energy, roughly 10 times higher. Second, individual grains in a grinding

9

wheel possess extremely negative rake angles. Though the average rake angle is about −30º, some individual grains might be as low as −60º. These very low rake angles indicate low shear plane angle and high shear strains, resulting in higher energy levels in grinding. Third, specific energy is higher in grinding because many of the individual grains are not involved in actual cutting. Because of having random positions and orientations in the wheel, some grains do not project far enough into the work to perform cutting. Three grain actions are recognized. (a) cutting, in which the grain projects far enough into the work to form a chip and accomplish cutting; (b) plowing, in which the grain projects into the work, but not that much far to perform cutting; rather, the work surface is deformed and energy is consumed without removing any material; and (c) rubbing, in which the grit touches the work surface during sweeping and rubbing friction occurs, thus consuming energy without any material removal. Nearly all (around 98%) of the total energy consumed in machining is converted into heat, resulting in a high temperature at tool-chip interface, usually over 600℃. The remaining 2% of energy is retained as elastic energy in the chip. Due to the size effect, high negative rake angles, and plowing & rubbing of the abrasive grits, the grinding process is characterized by high temperatures. Although most of the heat energy generated in conventional machining operations is carried off with the chip, much of the energy in grinding remains in the ground surface which results in high work surface temperatures. The high surface temperatures cause several possible damages, the first one being surface burns and cracks. Grinding burns are metallurgical damage immediately beneath the surface whereas surface cracks are perpendicular to the wheel speed direction. Both of these are indication of an extreme level of thermal damage to the work surface. The second harmful effect is softening of the work surface. Many parts are heat-treated to obtain high hardness prior to grinding. Due to the high grinding temperature, the work surface may lose some of its hardness. Third, residual stresses may form on the work surface because of the thermal effects. These stresses possibly result in decreased fatigue strength of the part (Groover, 2020). Therefore, dry grinding faces several technical problems, such as grinding wheel wear, thermal damage, poor surface integrity, loss of dimensional precision of the workpiece (Aurich et al., 2008).

1.2.4 Control of grinding temperature

The application of cutting fluids is an effective way in reducing thermal effects and controlling high work surface temperatures. Thus it provides better tool life, dimensional accuracy, product surface quality than the dry grinding. Quality in surface finish provides better aesthetic view, tribological properties, and corrosion resistance (Debnath et al., 2014). Cutting fluids that are used in grinding, are called grinding fluids. The functions of grinding fluids are: reducing friction, removing heat from the process, washing away chips, improving part surface finish,& dimentional accuracy, and reducing temperature of the work (Groover, 2020). If chips are not removed, they might clog the wheel and make it dull. Hence, during grinding the work, the only cutting operations occurring would be plowing and rubbing. Clogging increases cutting force, energy, and heat input to the workpiece (Irani et al., 2005). Grinding fluids typically are four types based on composition. They are water-based emulsions, straight oil, synthetic oil, and semi-synthetic oil. Straight oil provides best lublication but at the same time poor cooling characteristics (Groover, 2020). Soluble oils possess poor emulsion stability, thereby oils prone to separate out of the solution. Though semi-synthetics provide good lubrication for moderate and heavy-duty grinding, they tend to foam very easily which inhibits the heat transfer by limiting the amount of fluid in contact with the work and wheel (Irani et al., 2005).

Conventional approach to apply grinding fluids in the grinding zone includes flood cooling and high pressure cooling (HPC). These two methods use a huge amount of cutting fluids to the grinding area. Flood cooling is more commonly used method in grinding where no additional pressure is used to apply fluids. The application of flood cooling method in grinding has not been found effective in terms of reaching the grinding zone. Only 4 to 30% of the applied fluid could reach the grinding area because of an air barrier (Mandal et al., 2012). Air entrained around a rotating wheel periphery forms an air barrier that impedes fluid delivery. The grinding fluid must penetrate the air barrier to enter the grinding contact. At the surface, the entrained velocity is equal to the wheel velocity. With increasing distance from the surface, the velocity decreases and the pressure recovers. The fast-moving layer of air surrounding the wheel can't completely travel through the grinding contact, so it's deflected to the sides or flowed as rejected flow in the reverse direction.

With liquid coolant, the same thing happens (Rowe, 2013). Besides, for proper penetration of grinding fluid, fluid jet speed should be approximately 80–100% of wheel speed (Teicher et al., 2008). Also, the inherent high cost of disposal or recycling of the grinding fluid in flood cooling has become a major concern since environmental regulations get stricter worldwide (Mao et al., 2012). Another problem generates when the grinding temperature exceeds the fluid boiling temperature which in turn, vapors the fluid and hampers in reaching the grinding zone. HPC uses high pressure fluid flow to reach the grinding zone effectively. It creates a hydraulic wedge between the wheel and the workpiece that it can easily penetrate the air barrier around grinding wheel. As a result, it offers sufficient lubrication at tool-work interface thus reducing the friction significantly. It also provides effective removal of grinding chips from the grinding zone. In addition, HPC provides excellent chip breakability in grinding difficult to cut materials. Less machining temperature, surface roughness and better tool life is reported with HPC compared to flood cooling (Dhar et al., 2006; Zaman et al., 2020).

Traditional cutting fluids used in flood and HPC have environmental issues since they contain phosphorus, chlorine, sulfur or extreme-pressure additives for improving lubricity. They may come to human contact through aerial, skin, and ingestion. Among these three ways, skin contact is the main way and 80% of all occupational diseases are occured through skin exposure of workers to cutting fluids (Shokoohi et al., 2015). These chemicals are detrimental to worker health and cause environmental pollution. There is also a high cost associated with waste fluid treatment and it causes air pollution. It is estimated that the cost of cutting fluid is around 16% of the total machining cost. At high cutting temperatures, the cutting fluids may break to produce harmful gases. Besides, the disposal of used cutting fluids leads to water and soil contamination. The disposal cost of these fluids may be two to four times higher than their purchasing price because of expensive treatment prior to disposal (Debnath et al., 2014). When this toxic fluids comes in contact with skin, it causes dermatities, respiratory irritation, allergy, etc. Long term exposure to these fluids causesincreased risk of getting different types of cancer (Dhar et al., 2006).

The stringent legislation on health and environmental issues have been directed manufacturers to look for alternatives to the traditional cutting fluids that will be

environment friendly and cost saving as well. The continuous search and growing demand for eco-friendly alternatives had led to new alternatives such as dry grinding, solid lubricants, vegetable-based cutting fluids, cryogenic cooling with LN_2 or CO_2, and nanofluids. But dry machining lacks some advantages of cutting fluids. Dry grinding causes high temperature generation, high friction between the tool & work, rapid thermal damage of the ground surface, and reduced tool life. Compressed air cooling method suffers from low convective heat removal rate (Zaman et al., 2020). Cryogenic cooling with LN_2 or CO_2 could be a sustainable solution but it lacks the functionality of cutting fluids to remove chips from the grinding zone. One way to reduce wheel loading during grinding of soft Al alloys is to remove chips from the grinding zone. Besides, performance of cryogenic LN_2 assisted machining deteriorates at higher process parameters. Moreover, the cost associated with cryogenic cooling is very high and its handling & maintenance is difficult. Therefore, it is mainly used by researchers rather than in industrial applications (Mia & Dhar, 2019; Yasa et al., 2012). On the other hand, the use of solid lubricants is reported to fail to improve the tool performance leading to overheating of the grinding wheel and rapid wheel wear (Dhar et al., 2006). Vegetable based cutting fluids show inadequate oxidative stability and poor cooling ability. High speed machining requires the use of fluids with excellent cooling abilities (Kuram et al., 2013). Water can provide the best cooling performance along with low cost and environment friendliness. But water suffers from a slightly reduced lubricating performance that can be improved by suspending nanoparticles in the base fluid water.

Promising results in terms of Minimum Quantity Lubrication (MQL) grinding have been reported by many researchers with lower forces, decreased wheel wear, improved surface roughness, and residual compressive stresses in comparison with conventional flood grinding (Silva et al., 2007; Silva et al., 2005). MQL is a good trade-off between dry cutting and flood cooling. MQL grinding is also referred as near dry grinding. It uses a mixture of compressed air with less amount of oil in the form of fine drops forming a spray that is supplied to the cutting zone (Said et al., 2019). Here, cutting fluid consumption is very low, usually less than 100 ml/hour. This air-oil mixture is called aerosol. Aerosols are oil droplets dispersed in a jet of air and oil droplets are conveyed by the air directly to the cutting zone, thereby providing the required cooling and lubricating actions (Sadeghi et

al., 2009). Aerosols are generated through the atomization process which is a conversion of bulk liquids into spray or mist (Davim, 2008).

Improved surface roughness, diametric wear, grinding forces, and residual stress are reported with the MQL method in the grinding process owing to better lubrication of the grinding zone and better slipping of grain at the contact zone (Silva et al., 2007; Silva et al., 2005). Besides, MQL lubrication provides efficient lubrication, reduces grinding power and specific energy to a level comparable or superior to that of conventional soluble oil, also it significantly reduces grinding wheel wear (Hafenbraedl & Malkin, 2001). Because of so much lower fluid consumption than that of flood cooling, MQL grinding is considered a much more environmental friendly process. If the oil used in MQL is replaced with water, it will be even more environment friendly. Some other reasons are presented below to establish the necessity of using water instead of oils.

- For high cutting speed applications that generate high temperatures, coolant type cutting fluids are best suited (Groover, 2020). As discussed above, the grinding process is characterized by high temperatures. Since water has high specific heat and thermal conductivity relative to other liquids, it is used as the base cutting fluid here. These properties allow water to draw away heat from the operation and thus reduce the temperature of the cutting tool (Groover, 2020).
- High temperatures may cause oils to vaporize before they can lubricate.
- MQL with water provides better results than MQL without water in terms of workpiece surface roughness, roundness errors, and wheel wear (De Mello Belentani et al., 2014). Even it is stated that MQL with water as base fluid can be superior to conventional flood coolant (Do Nascimento et al., 2016). Also, studies established that MQL with water provides better cooling capacity than MQL without water, though with a slightly lower lubricating capacity based on the grinding force result (Mao et al., 2012). The lubricating property can be improved by adding nanoparticles to the water. The viscosity of the NFs increased approximately fourfold when compared to deionized water. Increased viscosity may aid in lubricating the contacting surfaces during actual grinding (Sinha et al., 2017). Therefore, water is selected as a base fluid in this research.

Nanofluids is the term coined by Choi (1995) to describe a new class of nanotechnology-based heat transfer fluids that exhibit thermal properties superior to those of their host fluids (Das et al., 2007). A nanofluid is a new fluid resulting from the dispersion of nanoparticles with a size of less than 100 nm into a base fluid. Nanoparticles used in nanofluids can be categorized into many types such as metallic, mixing metallic, non-metallic, carbon, and ceramic nano-particles (Said et al., 2019). Traditional heat transfer fluids such as water, oil, and ethylene glycol are commonly used as base fluids. A very small amount of nanoparticles can provide dramatic improvements in the thermal properties of host fluids when dispersed uniformly and suspended stably (Das et al., 2007). This enhanced thermal conductivity contributes to the machining processes significantly by quickly carrying the heat generated in the machining zone (Ghosh et al., 2015). Besides, this suspension of nanoparticles improves the viscosity of the resultant colloidal solution. It also exhibits enhanced lubrication (Sinha et al., 2017). The goal of nanofluids is to attain the highest possible thermal properties with the smallest possible concentrations (preferably< 1% by volume) by uniform dispersion and stable suspension of nanoparticles in host fluids (Das et al., 2007).

Zinc oxide (ZnO) nanoparticle is one of the most researched studies conducted due to their ability to be applied in various downstream applications (Mohan & Renjanadevi, 2016). It is the second most abundant metal oxide after iron. In addition, it is inexpensive, safe, and can be prepared easily (Kalpana et al., 2018). But the application of these nanoparticles in the manufacturing sector is still not very popular (Sinha et al., 2017). Physical and chemical behaviors of ZnO NPs can be easily altered by changing the morphology through different precursors or synthesis routes or different materials in producing the nanomaterial (Bala et al., 2014). ZnO NP has been proven to have antibacterial, antimicrobial, deodorizing, and non-toxic properties by several researchers. Also, it maintains cooling and lubricating properties at high temperatures that make it a suitable candidate for high temperature applications, such as grinding (Sinha et al., 2017). ZnO has been used in this research to be mixed with deionized water for producing nanofluids.

The NFs dynamic viscosity was found to be nearly four times that of DI water, which may have resulted in increased lubricity at the mating surfaces during grinding. ZnO

NFs based on water are effective at improving the grinding properties of Inconel 718. This is mostly due to the NFs' increased heat carrying capacity and better lubricity resulting in a decrease in the thermal load on the abrasive grits. The addition of NPs to DI water increased the thermal conductivity of the produced ZnO NFs. It revealed that heat convection may be improved further, particularly at greater grinding zone temperatures. Wear flattening of the grits is essentially non-existent, particularly in the case of ZnO. Grinding with ZnO NFs results in lower grinding forces, a lower friction coefficient, minimum debris clinging to the alumina grits, and a better ground surface. These beneficial observations are a result of the NFs' increased lubricating and spreading properties (Sinha et al., 2017).

Suspensions of nanoparticles in base fluids are produced by two methods; the two-step method and the single-step method. The two-step method first makes nanoparticles using nanoparticle processing techniques and then disperses them into base fluids. The single-step method makes and disperses nanoparticles into base fluids simultaneously. Most nanofluids containing oxide nanoparticles and carbon nanotubes are produced by the two-step process. On the other hand, the single-step technique is preferable to the two-step method for nanofluids containing high-conductivity metals (Das et al., 2007). However, the stability of the nanoparticles remains a concern for its users. Usually, nanoparticles become unstable with time which consequently affects their efficacy. Hence, this requires an appropriate methodology to be adopted to delay the clustering and agglomeration of the nanoparticles, thereby improving the stability of the nanofluids. Ultrasonication is performed after the addition of suitable surfactants into the base fluid. Surfactants are additives having high surface energy which helps in homogenizing and delaying the conglomeration of the nanoparticles.Surfactants act as wetting agents and reduce interfacial tension. Besides, the brownian motion of the nanoparticles significantly delays the agglomeration of the nanoparticles.Brownian motion is a random erratic motion that occurs as a result of the continuous collision between suspended nanoparticles and the molecules of the solvent (Sinha et al., 2017).

1.2.5 Problems in grindability of Al/SiC-MMC

The unique physical features and reliability of advanced composite materials have attracted interest in recent years. Composite materials have high hardness and retain it at high temperatures, are lightweight, and have excellent wear resistance (Shanawaz et al., 2011). Among composite materials, Metal Matrix Composites (MMCs) possess excellent mechanical properties such as high specific strength and wear resistance (Di Ilio et al., 2018). Because of their high specific characteristics, MMCs are widely used in the military, astronautics, and car industries. (Nas & Gökkaya, 2017). Although MMCs can be fabricated with near-net shape manufacturing, subsequent machining operations may be required to achieve desired dimensional tolerances as well as good surface finish. But MMCs shows poor machinability. Many machining operations result in reinforcing object's cracking, splintering, and pulling out. Conventional and unconventional methods such as turning, drilling, milling, electrical discharge machining, and laser machining can cause subsurface damage. Process such as grinding is crucial for the application of these materials to obtain smooth surface finish and damage-free surfaces (Zhong & Hung, 2000). But there is less information on the grindability of MMCs.

Silicon carbide and alumina are the most often used reinforcements for metal matric composite. The matrix phase is frequently composed of aluminum, titanium, and magnesium alloys (El-Gallab & Sklad, 1998). Among the MMC family, Al is selected as a matrix because of its excellent engineering properties, ease of production, and low-density capabilities (Nas & Gökkaya, 2017). Besides, It has a comparatively lower cost (Nandakumar & Rajmohan, 2018). But soft aluminum alloys have poor grindability due to chip adherence, thereby clogging the wheel. Grinding aluminum alloy-based MMCs is difficult as a result of this. Periodic dressing is required to avoid the aforementioned issues, which makes the grinding operation quite time consuming. Grinding forces rise as a result of grain blocking, which increases friction. Wheel clogging also reduces the effective life of the grinding wheel. It also causes high temperature generation, excess vibrations, greater surface roughness, redeposition, and low surface integrity. Aluminium alloys with silicon carbide reinforcement are a relatively new class of structural materials with high strength and modulus. If the reinforcements are in particulate shape, It's called particulate MMCs. Particulate MMCs exhibit lower anisotropy and higher ductility than

fiber-reinforced MMCs as well as better dimensional stability over corresponding unreinforced alloys. In addition, they are economically cheaper in terms of raw materials and fabrication process. Besides, Aluminum MMCs reinforced with silicon carbide (SiC) particles exhibit a yield strength increase of up to 20%, a greater modulus of elasticity,a lower coefficient of thermal expansion, and are more resistant to wear than the corresponding unreinforced matrix alloy systems (Okumus et al., 2012). As a result, Aluminium silicon carbide composite materials are presently employed in a variety of industries, including the automotive and aerospace industries. But, extremely abrasive SiC can cause quick tool wear (Shanawaz et al., 2011). Besides, Silicon carbide is difficult to grind due to its low fracture toughness, which makes it particularly susceptible to breaking (Nandakumar & Rajmohan, 2018). These are the problems that need to be addressed for the efficient and economic grinding of Al/SiC-MMC.

One way to solve the problems might be proper washing of the chips from the grinding zone. If chips are washed away properly, there will be less clogging of soft aluminum matrix on the wheel surface. Cutting fluids are employed to wash away chips as well as for reducing friction, removing heat from the process, improving part surface finish & dimentional accuracy, and reducing the temperature of the work (Groover, 2020). For applying cutting fluids, the flood cooling method is used as a traditional approach. But, flood cooling has been found ineffective in reaching the grinding zone. Only 4 to 30% of the applied fluid could reach the grinding area because of an air barrier (Mandal et al., 2012). Also, the inherent high cost of disposal or recycling of the grinding fluid in flood cooling has become a major concern since environmental regulations get stricter worldwide (Mao et al., 2012). Promising results in terms of Minimum Quantity Lubrication (MQL) grinding have been reported by many researchers with lower forces, decreased wheel wear, improved surface roughness, and residual compressive stresses in comparison with conventional flood grinding (Leonardo Roberto da Silva et al., 2007; L. R. Silva et al., 2005).

1.2.6 Summary of the review

Composite materials have high hardness and retain it at high temperatures, are lightweight, and have excellent wear resistance. Among the MMC family, Aluminum is

selected as a matrix because of its excellent engineering properties, low cost, ease of production, and low density capabilities. Although MMCs can be fabricated with near-net shape manufacturing, subsequent machining operations may be required to achieve desired dimensional tolerances as well as good surface finish. But MMCs show poor machinability. Grinding is crucial for the application of these materialsto obtain a smooth surface finish and damage-free surfaces. But Soft aluminum alloys have poor grindability due to chip adherence, thereby clogging the wheel. Grinding aluminum alloy-based MMCs is difficult as a result of this. Periodic dressing is required to avoid the aforementioned issues, which makes the grinding operation quite time consuming. One way to solve the problems might be proper washing of the chips from the grinding zone. If chips are washed away properly, there will be less clogging of soft aluminum matrix on the wheel surface. Cutting fluids are employed to wash away chips as well as for reducing friction, removing heat from the process, improving part surface finish & dimensional accuracy, and reducing the temperature of the work. Flood cooling has been found ineffective in reaching the grinding zone. Also, the inherent high cost of disposal or recycling of the grinding fluid in flood cooling has become a major concern since environmental regulations get stricter worldwide. Promising results in terms of Minimum Quantity Lubrication (MQL) grinding have been reported by many researchers with lower forces, decreased wheel wear, improved surface roughness, and residual compressive stresses in comparison with conventional flood grinding. Application of n-MQL comprises superior tribological and thermo-physical properties. High speed machining requires the use of fluids with excellent cooling abilities. Water can provide the best cooling performance along with low cost and environment friendliness. But water suffers from a slightly reduced lubricating performance that can be improved by suspending nanoparticles in the base fluid water. ZnO NP maintains lubricity at high temperatures which makes it a suitable candidate for high temperature applications, such as grinding. Therefore, the mentioned n-MQL seems to be a good candidate in grinding Al/SiC-MMC. To the best of the author's knowledge, no research has been carried out to evaluate the mentioned eco-friendly nanofluid through MQL in surface grinding of Al/SiC-MMC. The present work is motivated in fabricating an MQL set-up for surface grinding and evaluating the performance of MQL with ZnO-deionized water nanofluid compared to flood cooling in terms of the chip, grinding temperature, surface roughness, wheel wear, and grinding ratio.

1.3   Objectives of the study

Objectives of the present research are as follows:

i)   Design and fabrication of suitable MQL set-up for grinding that will make sure the continuous flow of nanofluid at a variable delivery rate towards the grinding zone during the grinding operation.

ii) Preparation of Zinc Oxide nanofluid mixed with Deionized water by ensuring uniform dispersion and proper stability of ZnO in the water to enhance the cooling property of nano-fluid.

iii) Optimization of the grinding parameters while grinding metal matrix composite under MQL.

iv) Experimental investigation on the roles of MQL with eco-friendly nano cutting fluid in respect of chip, grinding temperature, surface roughness, wheel wear, and grinding ratio in grinding of MMC at different process parameters.

v)   Development of a model to predict surface roughness using an Artificial NeuralNetwork while grinding Al/SiC-MMC under MQL with nano-cutting fluid.

1.4   Methodology

In order to achieve the objectives of this study, the set of methodologies that will be followed are as follows:

i)   A suitable MQL set-up has been designed and fabricated in such a way so that the variable MQL flow rate can be delivered continuously at the critical zones in grinding metal matrix composite.

ii) 0.5% volume of ZnO has been dispersed in base fluid (deionized water) with the help of ultra-sonication for few hours. Sodium dodecyl sulphate (SDS) surfactant has been added during the sonication for proper stability and homogenous dispersion of the NPs.

iii)   Experiments have been designed using central composite design and empirical models are developed to predict responses through RSM. The desired optimal combination for enhancing the grindability of Al/SiC-MMC have been selected using RSM based composite desirability approach.

iv)   Grinding has been performed by a Cubic Boron Nitride (CBN) grinding wheel at different process parameters using ecofriendly nano cutting fluid through MQL. Then grinding temperature and surface roughness have been recorded with the help of a thermocouple and surface roughness checker respectively. Grinding chips have been examined under SEM.

v)   A surface roughness model has been developed using ANN. Feed forward back propagation network structure has been used and the network has been trained by Levenberg-Marquardt equation.

1.5   Scope of the thesis

Chapter 1 starts with an introduction followed by a literature review that focuses on the importance of composite materials, particularly of the SiC reinforced Al-based MMC along with its poor machinability and way to improve its machinability. Then, the selection of the grinding wheel is discussed. After that, the effect of high temperature generation on grinding is briefly described along with measures for controlling temperature, the effect of conventional flood cooling and sustainable MQL cooling method, and techniques for improving MQL performance interms of nanofluids. Besides, a summary of the review, objectives of the study, and scope of the thesis are also included in chapter 1.

Chapter 2 consists of the design and fabrication of an MQL set-up, the preparation of the nanofluid, the experimental procedure and conditions, and the experimental results. Experimental procedure and conditions include the selection of material and grinding wheel and experimental set-up. Procedures for measurement of grinding zone temperature are discussed in experimental set-up. Experimental results present the results in terms of five responses.

Chapter 3 consists of two major parts; predictive modeling of surface roughness using ANN and optimization of process parameters selection. For the optimization, The

experimental runs are modeled first using central composite design (CCD). Based on the model, experimental runs are carried out for three factors and five responses. After the responses are taken, optimum parameters are obtained through multi-criteria optimization using desirability-based RSM.

Chapter 4 presents a discussion on the experimental results. Here, results are briefly discussed in respect of the five responses.

Chapter 5 contains conclusions and future recommendations. References are attached at the end.

Chapter-2

Experimental Investigations

2.1   Design and fabrication of an MQL set-up

The minimum quantity lubrication (MQL) system consists of an air compressor, fluid chamber, pressure controller, flow measuring device, mixing chamber, and nozzle. Compressed air was supplied by the compressor that is capable of generating up to 25 bar pressure. The capacity of the fluid chamber is 3 liter so that it can supply fluids for more than 3 hours with a 150 ml/hour flow rate. The fluid chamber is connected to the compressor from the inlet through a flexible pipe. Part of the compressed air is supplied to the fluid chamber through the inlet to facilitate fluid flow to the flow measuring device & to keep the fluid at constant pressure and then to the mixing chamber through a flexible pipe. The rest of the compressed air is supplied to the mixing chamber. The mixing chamber is used to mix cutting fluid and compressed air. It has two inlet ports and one outlet port. Through the inlet ports, water and compressed air enter the mixing chamber. The outlet port contains a grinding nozzle. In the mixing chamber, both the cutting fluid and compressed air pass through a filter that consists of 5 small holes of 1mm diameter before being mixed together. These small holes break the fluids into smaller droplets. After mixing, they are further broken as they pass through the nozzle containing a 0.5 mm outlet. Sudden expansion at the inlet port and contraction at the outlet port of the mixing chamber results in turbulence in the airflow and ensures proper mixing of air with cutting fluid in the chamber.

The first step of the experimental work involves designing and fabrication of a suitable MQL delivery system for the grinding process. For this reason, two grinding nozzles and one mixing chamber involving some modifications are designed and fabricated. The parameters that were considered in designing the nozzles and the mixing chamber are listed in Table 2.1 along with their levels. To choose the best level, some trial runs were performed while keeping the machining parameters unchanged (150 ml/hour fluid flow and 8 bar air pressure). Based on the trial runs, final parameters were chosen for fabrication. It was found

that keeping the same diameter for both the nozzle inlet and mixing chamber outlet, 13 mm in this case, provides better jets in terms of coherency. On the other hand, different diameters for the nozzle inlet (19 mm) and mixing chamber outlet (13 mm) increased the turbulency of the fluid jets. Besides, a tapered shape nozzle performed better than the round shaped nozzle. Tapered shaped nozzle facilitates smooth contraction of the fluid from the 13 mm inlet to the 0.5 mm nozzle outlet. In case of the mixing chamber, four holes of diameter 1 mm each were drilled through which pressurized air and nanofluid enters mixing chamber. The holes were made at positions similar to the 12,3,6, and 9 positions of a clock. Then, one hole is added at the center. It was found that five holes produced better fluid flow. Selected levels are also shown in Table 2.1 in the rightmost column.

Table 2.1 Factors considered in designing MQL applicator

Sl. No.	Factors	Experimental levels		Selected level
1	Inlet diameter of the nozzle	19 mm	13 mm	13 mm
2	Number of holes through which pressurized air enters the mixing chamber	4	5	5
3	Number of holes through which nanofluid enters the mixing chamber	4	5	5
4	Type of nozzle outlet	Round	Tapered	Tapered

(a) Isometric view

(b) Mixing chamber with nozzle
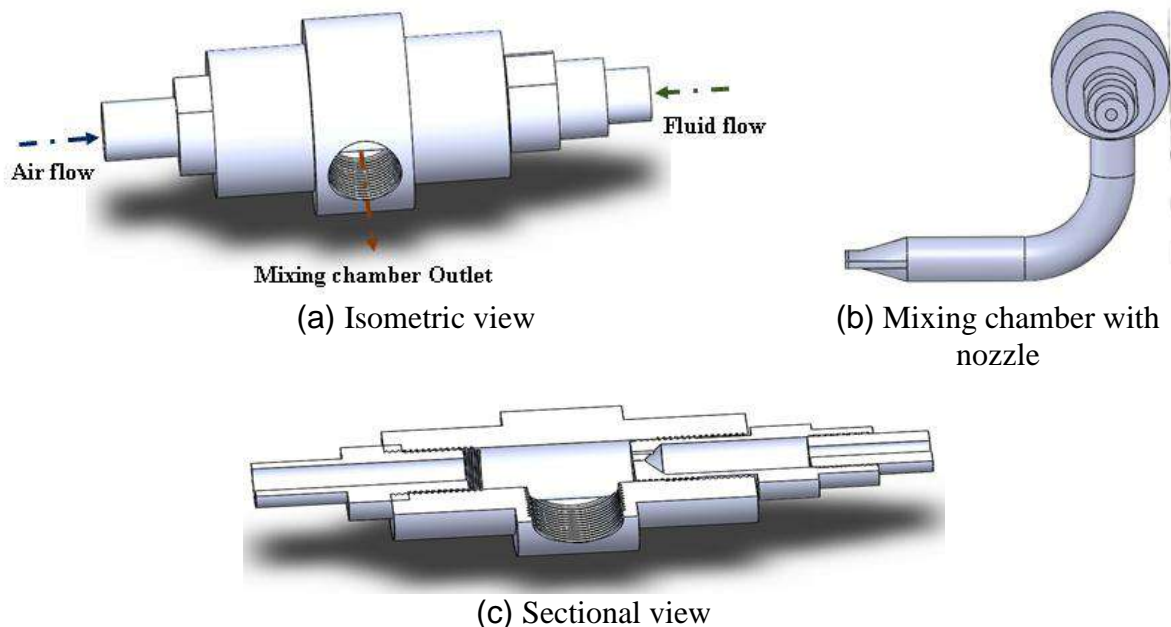
(c) Sectional view
Fig.2.1 Different views of the mixing chamber

The isometric view and sectional view of the mixing chamber and the mixing chamber with a nozzle are presented in Fig. 2.1. Here, water and compressed air come to the mixing chamber from two opposite ends for better mixing. The grinding nozzle is attached to

the mixing chamber with the outlet port in a direction perpendicular to the direction of water-air inlets.

Nozzle design and its position greatly influence productivity, workpiece surface quality, and wheel wear (Bianchi et al., 2013). The spraying direction of the MQL nozzle has a significant impact on the application of the nanofluid mist and subsequent lubrication and cooling of the grinding zone, according to experimental data. In order to achieve the best grinding results, the nozzle should be placed angularly toward the wheel at approximately 10–20° to the workpiece surface. Nanofluid mist penetration into grinding zones can be enhanced by increasing air pressure and spraying distance. Grinding forces, surface roughness, and grinding temperature decrease when air pressure is increased, and grinding performance is superior in shorter spraying distances (Mao et al., 2013; Tawakoli et al., 2010). The nozzle used in this researchis angular at 10° to the workpiece surface and is placed 30 mm away from the grinding wheel.

2.2   Preparation of nanofluid

Purified deionized water has been used in this research instead of tap water to eliminate any possible contamination which may significantly change the nanofluid characteristics (Sinha et al., 2017). ZnO nanoparticles bought from Guangzhou Hongwu Material Technology Co., Ltd., china have been used to make nanofluids by mixing with deionized water. These NPs are antibacterial, antifungal, and antifouling agents. A quick overview of the ZnO nanoparticles applied is presented in Table 2.2.

Table 2.2 Physical properties of the ZnO NPs

Appearance	Particle Size (nm)	Morphology	Specific surface area (m^2/g)	Density (g/cm^3)	Melting point	Purity	Grade	Water solubility
White solid powder	20-30	Spherical	50	5.61	1975°C	99.8%	Industrial	Insoluble

In this research, ZnO suspensions have been produced using two-step method. Water soluble Sodium dodecyl sulphet (SDS) [$CH_3(CH_2)_{10}CH_2OSO_3Na$] is used as a surfactant. At first, commercially available industrial grade ZnO nanoparticles and SDS have been collected. Then, nanoparticles and SDS are weighted using a high-precision digital balance to get the desired amount to be mixed with base fluid. For this purpose, aluminum foil paper

25

was put into the scale and the calibration button was pressed to eliminate the weight of the aluminum foil paper. The required mass can be calculated from the following equation:

$$\% \text{ volume concentration } = \frac{\frac{m_{ZnO}}{\rho_{ZnO}}}{\frac{m_{ZnO}}{\rho_{ZnO}} + \frac{m_{water}}{\rho_{water}}} \quad \text{.. (2.1)}$$

where, m_{ZnO} is the mass of the ZnO nanoparticle to be determined in kilograms, ρ_{ZnO} is the density of water in kilograms per cubic meter, m_{water} is the mass of the base fluid water in kilograms, and ρ_{water} is the density of water in kilograms per cubic meter. Nanofluids containingthree distinct volumes of ZnO nanoparticles (0.01, 0.1, and 0.5 vol.%; S-1, S-2, and S-3, respectively) were prepared for stability testing. The calculated amount of ZnO nanoparticles and SDS are listed in Table 2.3 for different volume concentrations.

Table 2.3 Chemical analyze of ZnO nanoparticles and SDS for different volume concentrations

Volume of deionized water (ml)	Mass of ZnO NPs (g)	Volume concentrations of ZnO NPs (vol %)	Mass of SDS (g)
100 ml	0.056	.01	0.0056
100 ml	0.56	0.1	0.056
100 ml	2.82	0.5	0.282

Due to severe sedimentation and aggregation of nanoparticles, mixing nanoparticles in base fluid is difficult. Hence, This has been made in two steps. At first, ZnO has been poured in deionized water. Then, 'Magnetic stirring' was performed for half an hour with a rotational speed of 700 rpm to mix the nanoparticle with the water followed by 30 minutes of Ultrasonication bath using a 2510 BRANSON ultra-sonicator operated at 20-25 kHz frequency with 150 W of output power being generated to disperse the nanoparticles uniformly for preventing the agglomeration of the fluid. Ultrasonicator create such vibration that the nanoparticles cannot sustain its destructive effect. Therefore, it breaks down into smaller particles and produces proper dispersion that in turn provides long stability to the nanofluids. Nanofluids with three different volume concentrations of ZnO nanoparticles were produced as shown in Table 2.3. Nanofluids are then stored inside completely transparent glassy containers in a completely stagnant condition for about 24 h for evaluating their stability conditions. After 24 hours, the stability of nanofluids was observed through visual inspection. 0.5% volume concentration of ZnO showed better results in terms of stability. Therefore, 0.5% ZnO concentration has been selected for this research experiment. Fig. 2.4 shows nanofluid samples after preparation and after 24 hours, respectively.

(a) Deionized water   (b) ZnO nanoparticles   (c) SDS

Fig. 2.2 Materials used for producing nanofluids.

(a) Mass measurement using high precision digital balance

(b) Magnetic stirring (30 minutes)

(c) Ultrasonic bath (30 minutes)

Fig. 2.3 Steps to produce nanofluids

(a)   (b)

Fig. 2.4 Stability of nanofluids after (a) preparation and (b) 24 hours

2.3 Experimental procedure and conditions

2.3.1 Selection of material and grinding wheel

Al/SiC-MMC is a newer type of structural material with excellent strength and modulus. Furthermore, they are less expensive in terms of raw materials and manufacturing processes. As a result, this is now used in a wide range of industries, including automotive and aerospace. A rectangle-shaped workpiece composed of SiC reinforced Aluminum-based metal matrix composite with dimensions of 160 mm length, 115 mm width, and 80 mm thickness was used in this investigation. Its main constituents are Al, Si, Cu, Fe, and Li. Constituents with volume percentage values are listed in Table 2.4. The grinding wheel had 227 mm outer diameter and 25 mm width before performing the process. Figure 2.5 provides a pictorial view of the workpiece and the grinding wheel.

Table 2.4 Workpiece constituents in volume percentage

Al	Si	Cu	Fe	Others
84.7	8.22	1.97	0.42	4.69

(a) Al/SiC-MMC workpiece   (b) CBN grinding wheel

Fig.2.5 Photographic view of Al/SiC-MMC workpiece and grinding wheel

2.3.2 Experimental set-up

A horizontal spindle surface grinder (2.8 kw, Model: M7120A) along with a vitrified bonded CBN grinding wheel was used to perform surface grinding in this research. The grinder is equipped with a magnetic chuck to hold the work on the machine table by exerting a magnetic force on it. But a magnetic chuck can hold the work properly if the work is made

of magnetic material such as iron or steel.Since the workpiece used in this research is Al/SiC-MMC, it could not be held with the magnetic chuck. Rather, it was held in a vise that was fastened to the table. The wheel was dressed properly before the experimental run. After completing experimental runs for each of the cooling environments, the wheel was dressed again. Up grinding was performed during the whole experiment. For flood cooling, 10% diluted water-soluble oil (Aquatex 3180) was used as a coolant. This fluid was applied using the nozzle that comes with the surface grinder machine having a 1 mm outlet diameter. In the case of MQL, The MQL set-up mentioned in section 2.1 was used to supply air-fluid mixture during the process. Table 2.5 lists the summarized conditions for experimental runs.

Table 2.5 Experimental Conditions

Grinding mode	: Horizontal spindle with reciprocating worktable surface grinding
Machine tool	: Horizontal Spindle Surface Grinder (2.8 kw, Model: M7120A)
Grinding wheel	: Vitrified CBN
Spindle speed	: 1500 and 3000 rpm
Work speed	: 6 m/min
Infeed	: 10,15,20,25,35 and 40 μm
Cutting conditions	: Flood cooling and MQL
Cutting fluid	: 10% diluted water soluble cutting oil
MQL cutting fluid	: Eco-friendly ZnO nanoparticle dispersed deionized water
Nano fluid flow rate	: 150 ml/hr
Air pressure in MQL	: 8 bar
Workpiece material	: Al/SiC-MMC
Nozzle angle	: 10° to the horizontal
Nozzle position	: 30 mm from the wheel
Dresser	: Diamond wheel dresser
Dressing depth	: 1.0 mm
Dressing speed	: 3000 rpm

Grinding chips were collected during the experiment from all of the experimental runs. A rectangular shaped white paper coated with grease was held near the wheel during the operation so that flying chips got trapped in it. On average, 10 chips from each experimental run were trapped on the paper. The chip-containing papers were then carefully pinned on a white foam board. Since grinding chips are small in size, these were observed through a SEM and captured. Chips from 10 experimental runs were observed through SEM. Irregular & fragmented chips were excluded from further considerations to get significant insights about the chip types.

In this experiment, grinding zone temperature was measured using an iron-constantan single pole embedded thermocouple technique. A J-type thermocouple was made using constantan wire. A rectangular slot of 25 mm depth and 2 mm wide was cut on the workpiece

through wire cut Electrical discharge machining. The slot is cut to place the constantan wire head through the slot so that it touches the rotating wheel, thereby being the hot zone during the grinding operation. Mica sheets are employed in several places between the bench vice & workpiece and between constantan wire & workpiece for proper insulation. The opposite end of the constantan wire was connected to the multimeter. The iron wire was placed away from the rotating wheel and between the workpiece & mica sheet to work as a cold zone during operation. The opposite end of the iron wire was connected to the multimeter to complete the circuit. At the time when the grinding wheel touches the constantan wire, some voltage was generated due to the seeback effect. This voltage was shown in a multimeter in a milivolt (mV) unit. A schematic diagram of temperature measurement at the grinding zone is presented in Fig. 2.7.
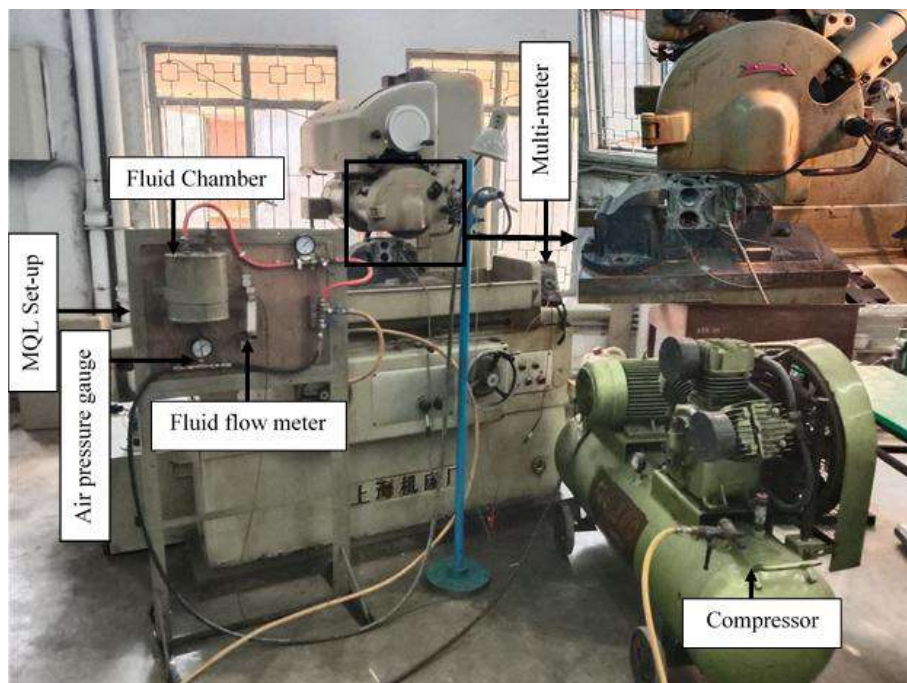
Fig. 2.6 Photographic view of the experimental set-up
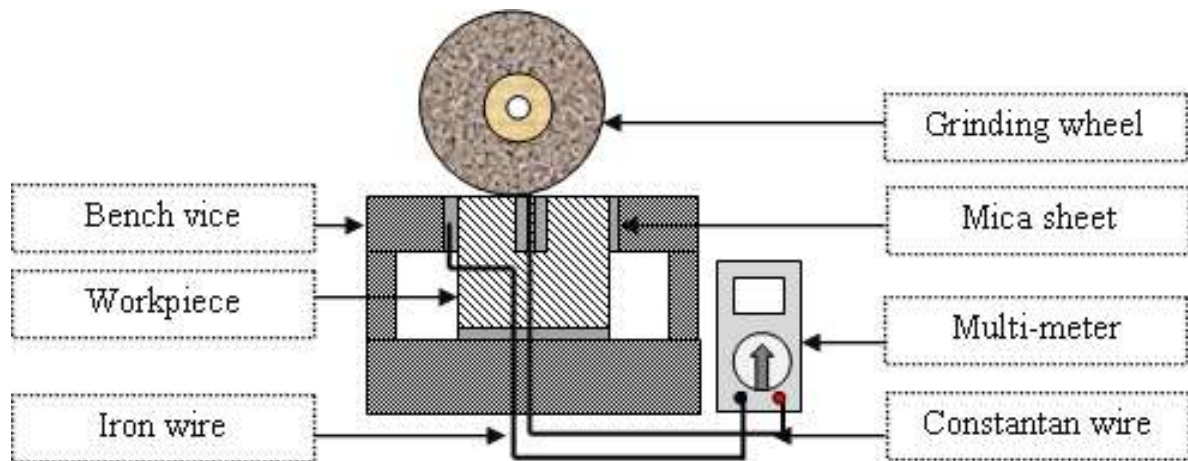
Fig. 2.7 Schematic view of grinding zone temperature measurement technique

Calibration was performed to convert the voltage generated (mV) to the corresponding temperature values (°C). Therefore, a small part of around 20 mm in length, 10 mm in width, and 4 mm in height were cut from the workpiece. To join it at one end with a constantan wire, brazing was first tried. But, the workpiece could not withstand the high temperature generated during brazing since the aluminum alloy is present as matrix material and hence it melted. The join was then made mechanically. The other ends of the work part and constantan wire have been connected to a digital multi-meter (SANWA digital multimeter-CD772). The joined junction of the work-constantan wire and a reference thermocouple (chromel-alumel) were placed contiguous to each other on a carbon block. The carbon block was placed on a radiant heater. The heater was then turned on and the joint served as a hot junction of the thermocouple. Thermoelectric voltage is generated at the thermocouple which was shown by the multi-meter. The temperature (°C) of the hot junction was measured by the reference chromel alumel thermocouple and the temperature value in degreesCelsius was shown by a digital thermometer (Eurotherm, UK). Corresponding voltage and temperature were recorded during heat application. The photographic view of the set-up for calibration has been shown in Fig. 2.8.
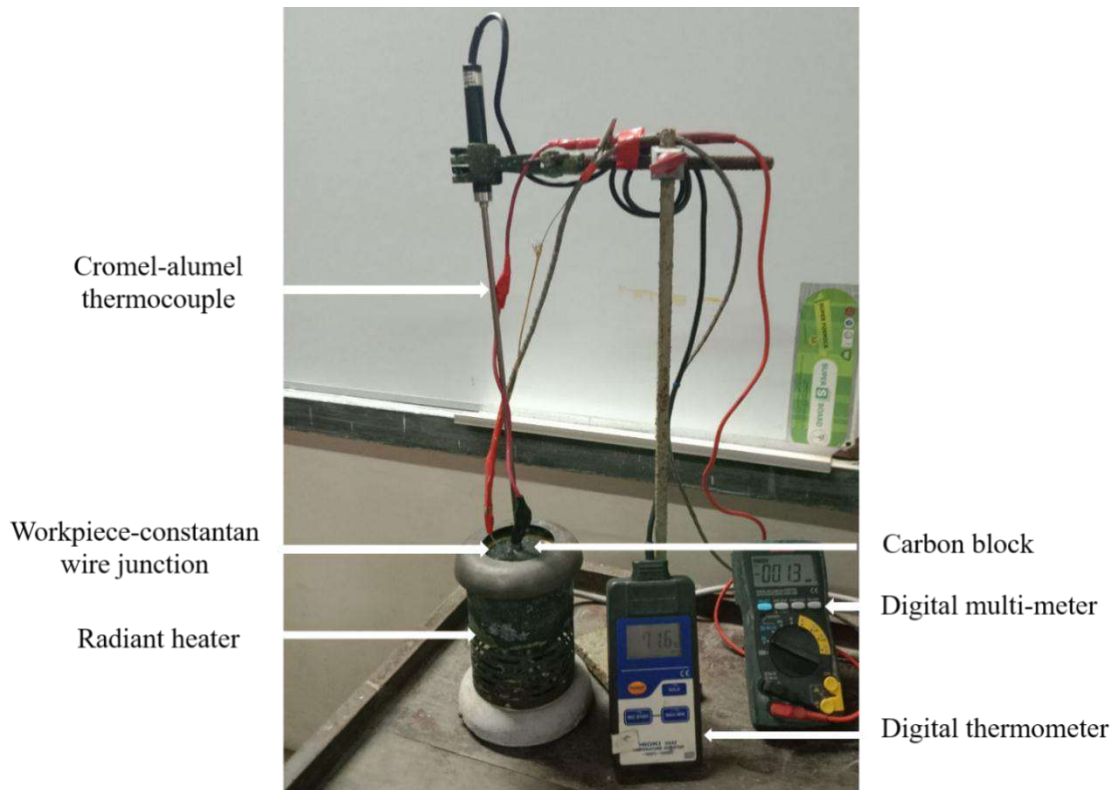
Fig. 2.8 Scheme of calibration of present tool-work thermocouple

Thermoelectric voltages (mV) along with corresponding temperature values for this workpiece are plotted in Fig. 2.10. Almost linear relationship is found with more than 99% accuracy. A regression equation is established to predict the corresponding temperature values from voltages.

Temperature (°C) for Al-based MMC= 18.28 * Voltage (mV) + 66.256 ....(2.2)
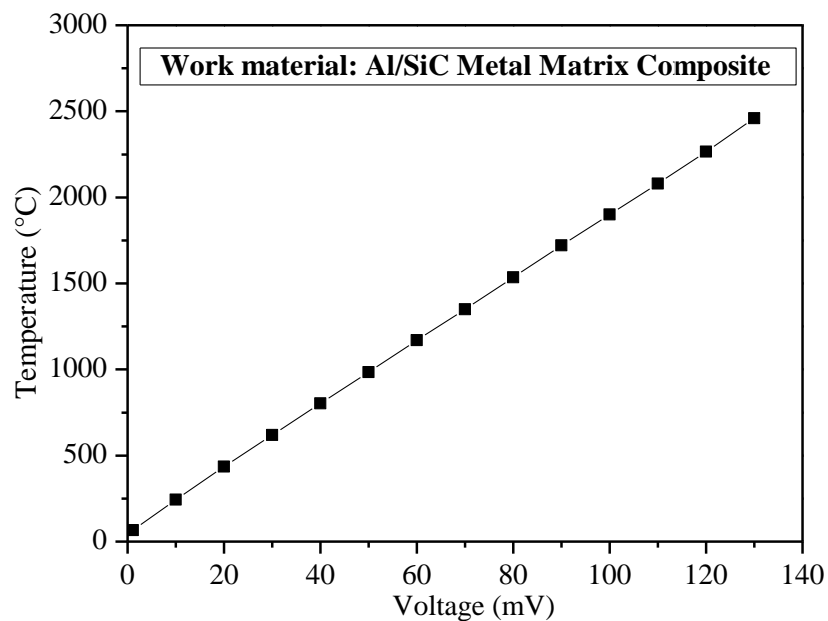
Fig. 2.9 Calibration curve for Al/SiC-MMC

2.4   Experimental results

2.4.1 Chip morphology

Along with flood cooling and nMQL, dry grinding of Al/SiC-MMC was initially beyond the scope of this research. But, dry grinding of Al/SiC-MMC with CBN grinding wheel was not successful because of rapid clogging of the grinding wheel with soft aluminum matrix. Chips deposition in the grinding wheel causes wheel clogging. Wheel clogging reduces tool life and makes the wheel dull (Agarwal, 2019). Fig. 2.10 to 2.13 presents SEM images of grinding chips at different magnifications and parameters. Chip types are listed in Table 2.6 which indicates that no ripping and melting type chips were observed in any of the experimental runs. Knife and slice type chips dominate the nMQL and flood cooling environment, respectively. At higher spindle speed and higher infeed, slice chips are more common for both of the cooling environments. The occurrence of slice chips with flood cooling or higher speed-infeeds indicates wheel loading in these scenarios. As a result, it requires frequent dressing during flood cooling for this work-wheel combination. Hence, grinding at higher speed-infeed both for flood & nMQL and flood cooling is ineffective for grinding Al/SiC-MMC with a CBN grinding wheel. Therefore, these parameters are not suggested. Grinding with MQL is thus recommended for the respective workpiece-wheel combination.

Environment	Magnification		
	100x	200x	500x
Flood Cooling			
n-MQL			
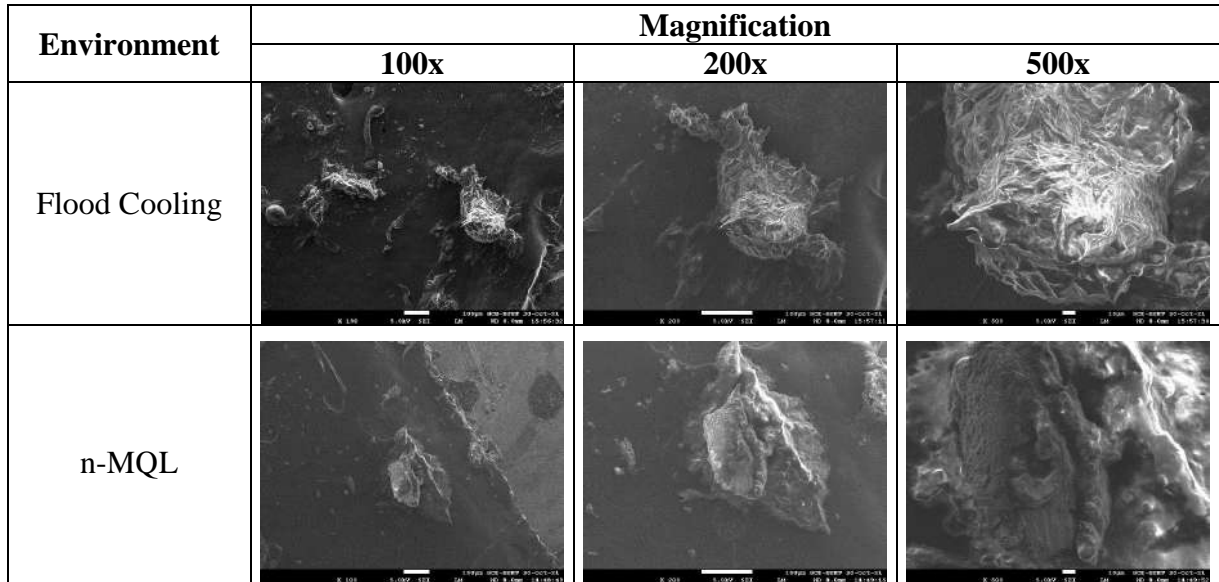
Fig.2.10 SEM views of grinding chips under flood and n-MQL conditions at 10 μm infeed and wheel speed 1500 rpm while grinding Al/SiC MMC

Environment	Magnification		
	100x	200x	500x
Flood Cooling			
n-MQL			
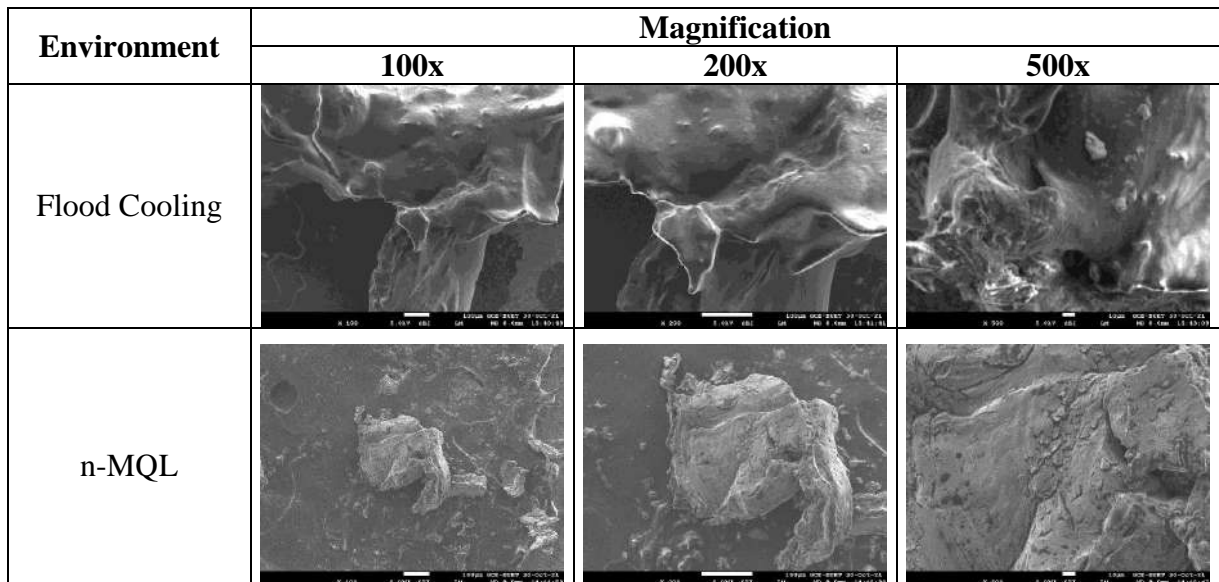
Fig.2.11 SEM views of grinding chips under flood and n-MQL conditions at 40 μm infeed and wheel speed 1500 rpm while grinding Al/SiC MMC

Environment	Magnification		
	100x	200x	500x
Flood Cooling			
n-MQL			
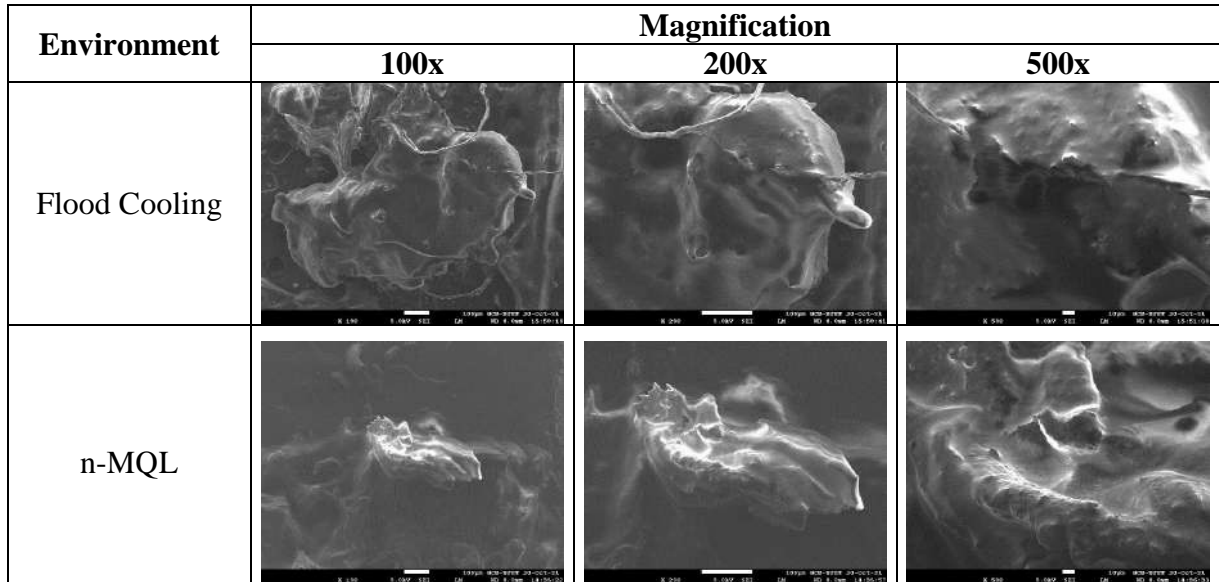
Fig.2.12 SEM views of grinding chips under flood and n-MQL conditions at 10 μm infeed and wheel speed 3000 rpm while grinding Al/SiC MMC

Environment	Magnification		
	100x	200x	500x
Flood Cooling			
n-MQL			
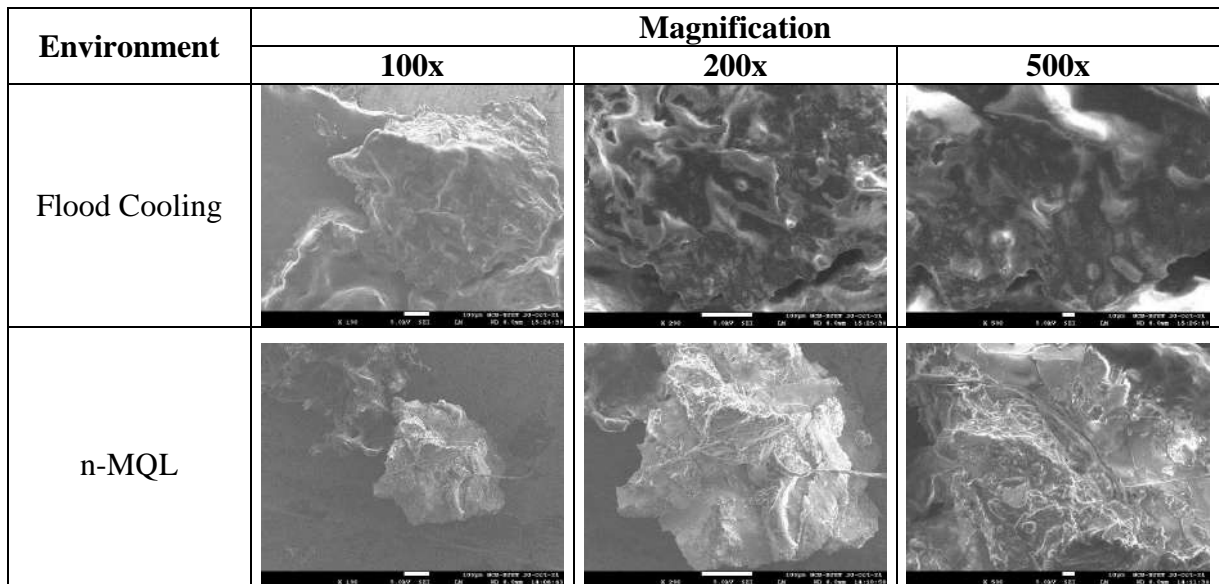
Fig.2.13 SEM views of grinding chips under flood and n-MQL conditions at 40 μm infeed and wheel speed 3000 rpm while grinding Al/SiC MMC

35

Table 2.6 Chip types for different input parameters

Serial	Spindle speed	Infeed	Environment	Chip type
1	1500	10	Flood	Knife, Slice
2	1500	40	Flood	Slice
3	3000	10	Flood	Slice
4	3000	25	Flood	Slice
5	3000	40	Flood	Slice
6	1500	10	nMQL	Knife
7	1500	40	nMQL	Knife, Shearing
8	3000	10	nMQL	Knife
9	3000	25	nMQL	Shearing
10	3000	40	nMQL	Slice

2.4.2 Grinding zone temperature

The values of the grinding zone temperature for different spindle speeds, infeed, and environments are plotted in degrees Celcius and are shown in Fig. 2.14. From Fig. 2.14, it is observed that flood cooling generates temperatures ranging between 700 to 1584°C for grinding the workpiece material. On the other hand, ZnO-deionized water based nMQL drastically reduced the temperature to 540 to 1188°C, thereby 25% reduction in temperature for nMQL than flood cooling (for 3000 rpm spindle speed and 40 μm infeed). nMQL produced comparatively lower temperature than the corresponding flood cooling temperature. This may be because of the effective lubrication of the nMQL method in reaching the grinding zone and enhanced thermal conductivity of the ZnO-deionized water nanofluid. A 33% increase in thermal conductivity is reported after suspending ZnO NPs in water where the thermal conductivity of water and ZnO is 0.578 and 100 W/m-K respectively (Sinha et al., 2017). Besides, higher temperatures are observed at higher infeeds and/or higher spindle speeds, for both the flood cooling and nMQL approach.
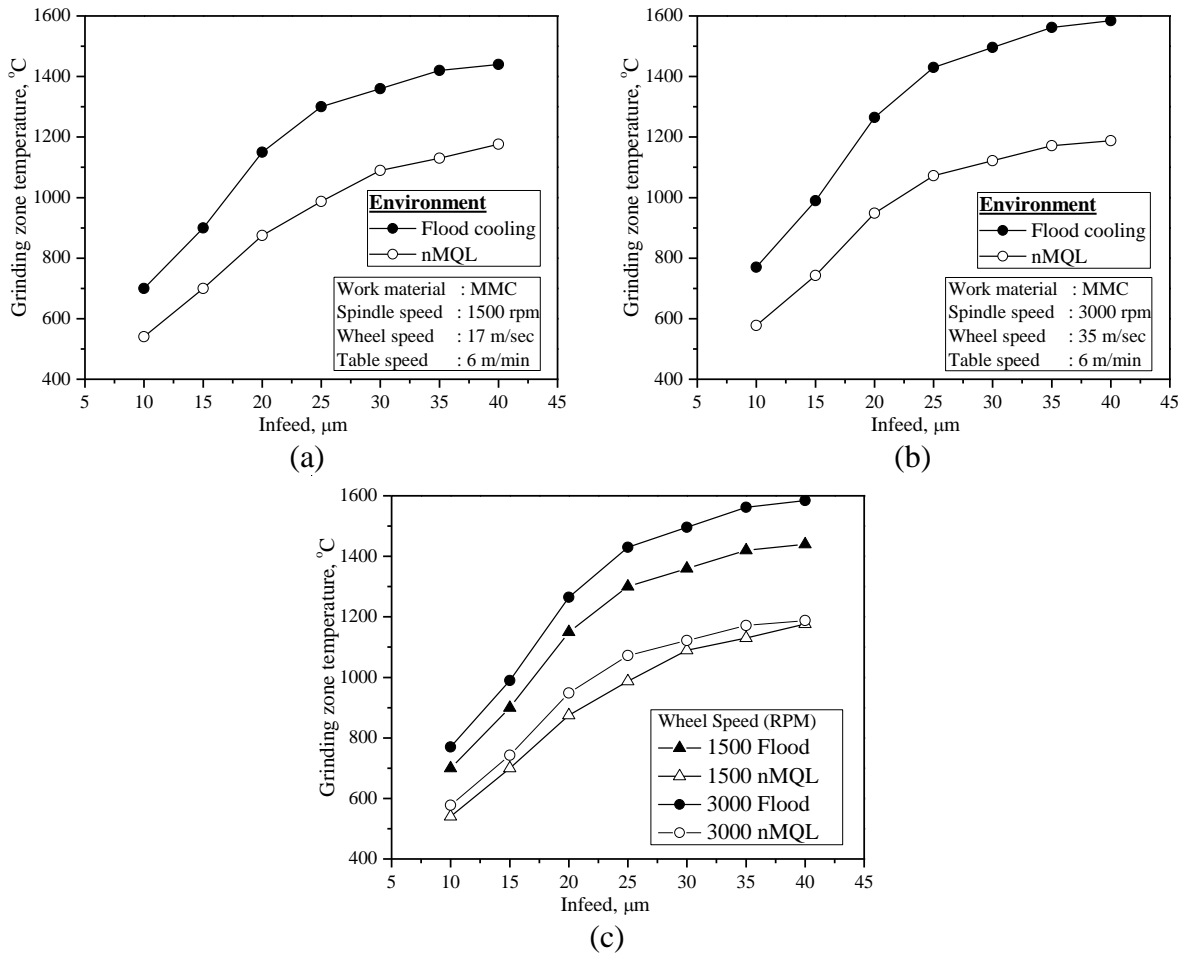
Fig. 2.14 Variation of grinding temperature with infeed under flood and nMQL conditions for (a) 1500 rpm, (b) 3000 rpm, and (c) 1500 and 3000 rpm spindle speed

2.4.3 Surface roughness

Machined components' surface topography can be characterized by their surface roughness. It is clearly influenced by cutting parameters, work-tool material, tool geometry, and statistical variance during the machining process. Surface roughness determines the quality of finish. It has a vital role in various engineering applications. Reasonable surface finish is always appreciated to improve tribological aspects and aesthetic appearance whereas excessive surface finish is responsible for higher machining cost. The degree of smoothness of a machined component's surface is determined by the amount of roughness, waviness, and defects created because of the machining process (Chandrasekaran & Devarasiddappa, 2014). Fig. 2.15 plots the values of surface roughness (R) with respect to corresponding infeed values for different spindle speed and environment. Infeed values are plotted in X-axis and the corresponding roughness values are plotted in Y-axis. It is clear from the figure that

nMQL produced lower surface roughness than flood cooling at any speed-infeed combination. Higher infeeds and/or lower spindle speeds produced higher roughness values.

(a)

(b)

(c)

Fig. 2.15 Variation of surface roughness with infeed under flood and nMQL conditions for (a) 1500 rpm, (b) 3000 rpm, and (c) 1500 and 3000 rpm spindle speed

2.4.4 Wheel wear

The CBN grinding wheel used in this research has a 227 mm outer diameter and 25 mm thickness. Wheel diameter was measured before and after each of the experimental runs. From the diameter difference, tool wear is calculated using the equation below.

$$Q_s = 2\pi b \Delta r \quad\text{.. (2.3)}$$

where Q_s is volumetric wheel wear, Δr is the radius reduction of the grinding wheel, and b is the width of the grinding wheel. The diameter difference was measured using a slide caliper. Tool wear is plotted in Fig. 2.16 for different input parameters.
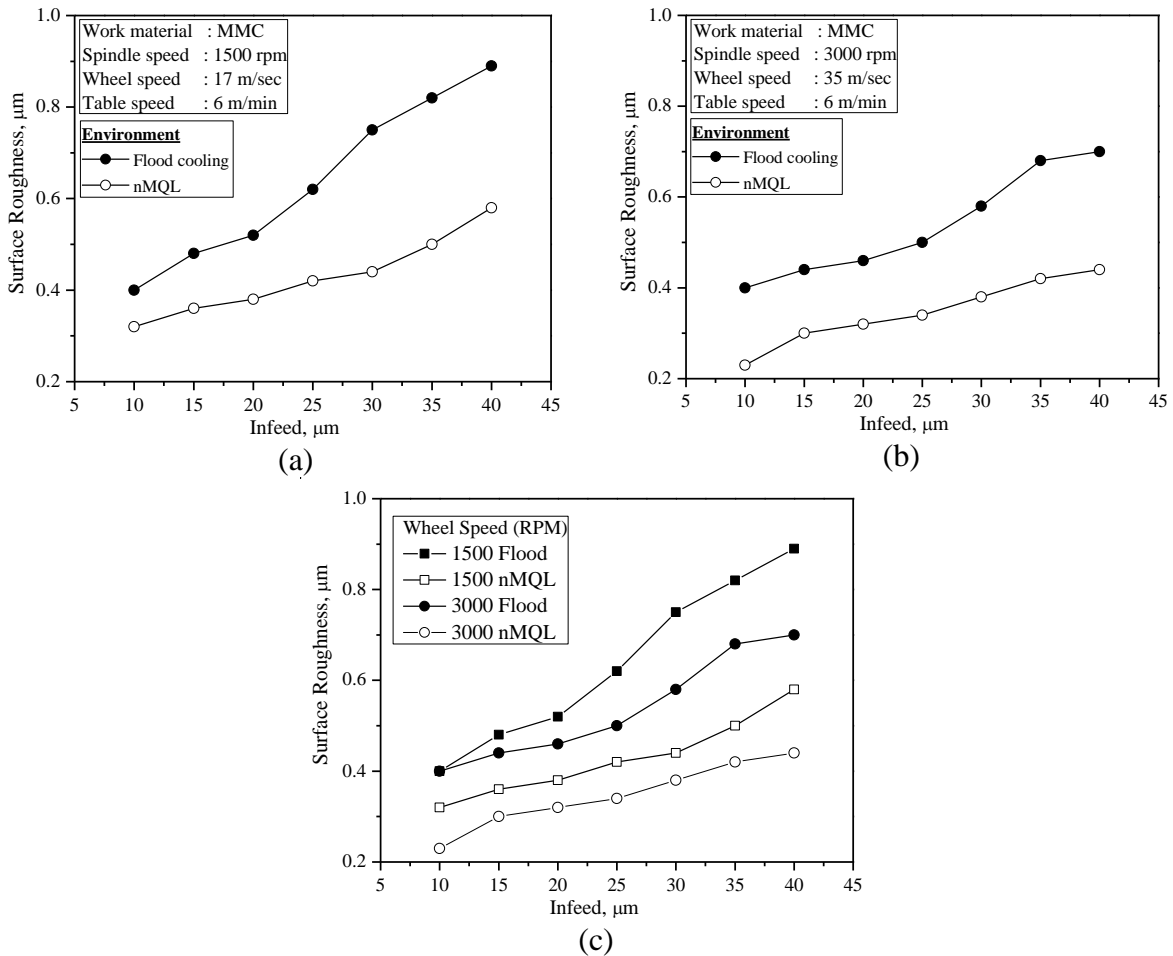
Fig. 2.16 Variation of wheel wear with infeed under flood and nMQL conditions for (a) 1500 rpm, (b) 3000 rpm, and (c) 1500 and 3000 rpm spindle speed

Fig. 2.16 indicates that higher infeed and/or lower spindle speed values produced greater wheel wear regardless of the cooling environment. Flood cooling generated rapid wheel wear when infeed was increased beyond 30 μm. For any spindle speed-infeed combination, nMQL produced less wear than flood cooling.

2.4.5 Grinding ratio

Grinding ratio (G) is the ratio between the material removal of the workpiece and the wear of the grinding wheel. It is one of the measures to evaluate grindability (Inasaki & Nakayama, 1986). In addition, it is the most widely used parameter to evaluate the performance of grinding wheel (Kwak & Ha, 2002). Grinding ratio can be calculated from the equation below.

$$G = \frac{Q_w}{Q_s}$$ .... (2.4)

39

$$Q_{w\ =bLt} \hspace{0.5em} \text{..} \hspace{0.5em} (2.5)$$

$$Q_s = 2\pi b\Delta r \text{...} \hspace{0.5em} (2.6)$$

where Q_w is volumetric workpiece removal, Q_s is volumetric wheel wear, L is the total length of the workpiece, Δr is the radius reduction of the grinding wheel, t and b are the depth of cut and width of the grinding wheel, respectively. Figure 2.17 shows the grinding ratio for different wheel speed, infeed, and environment.
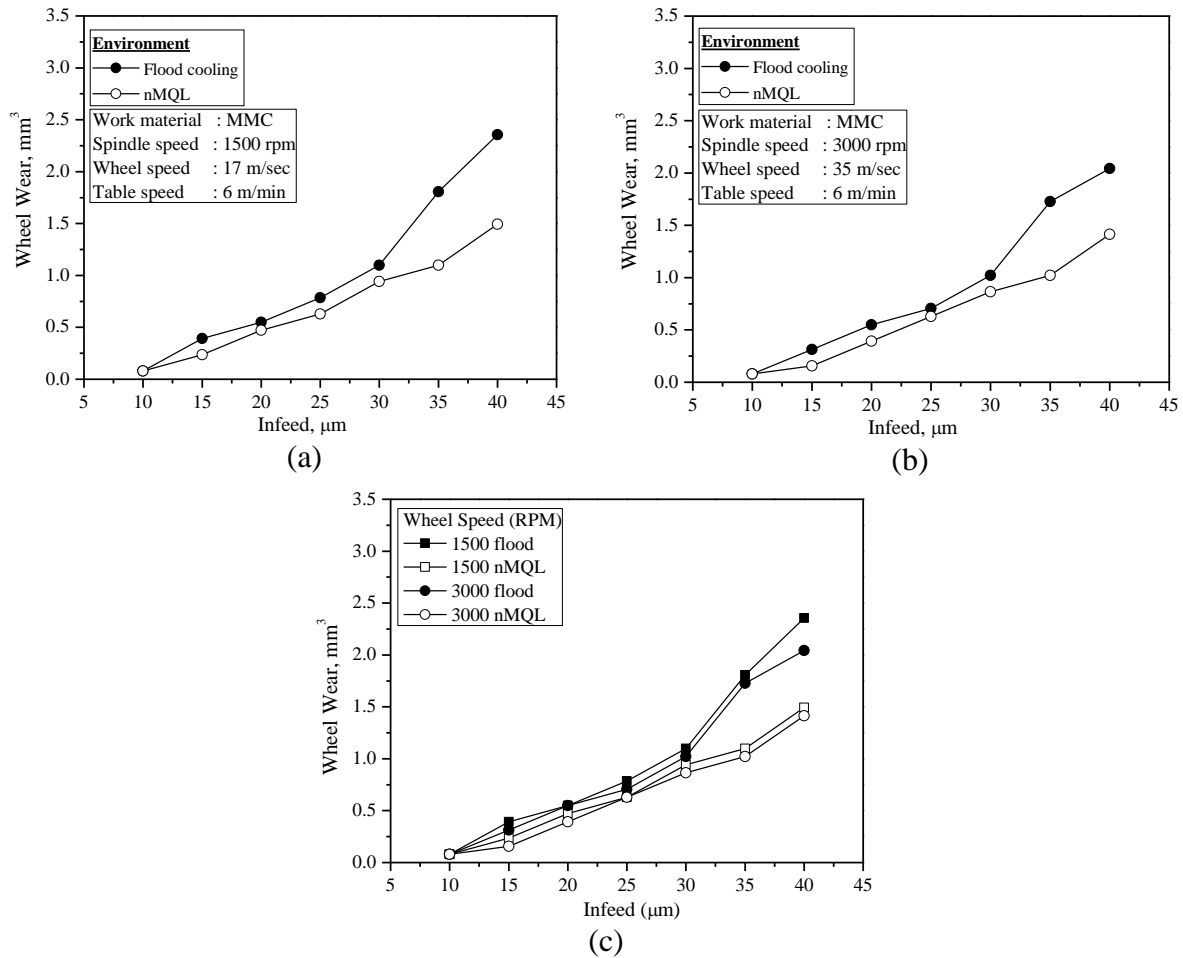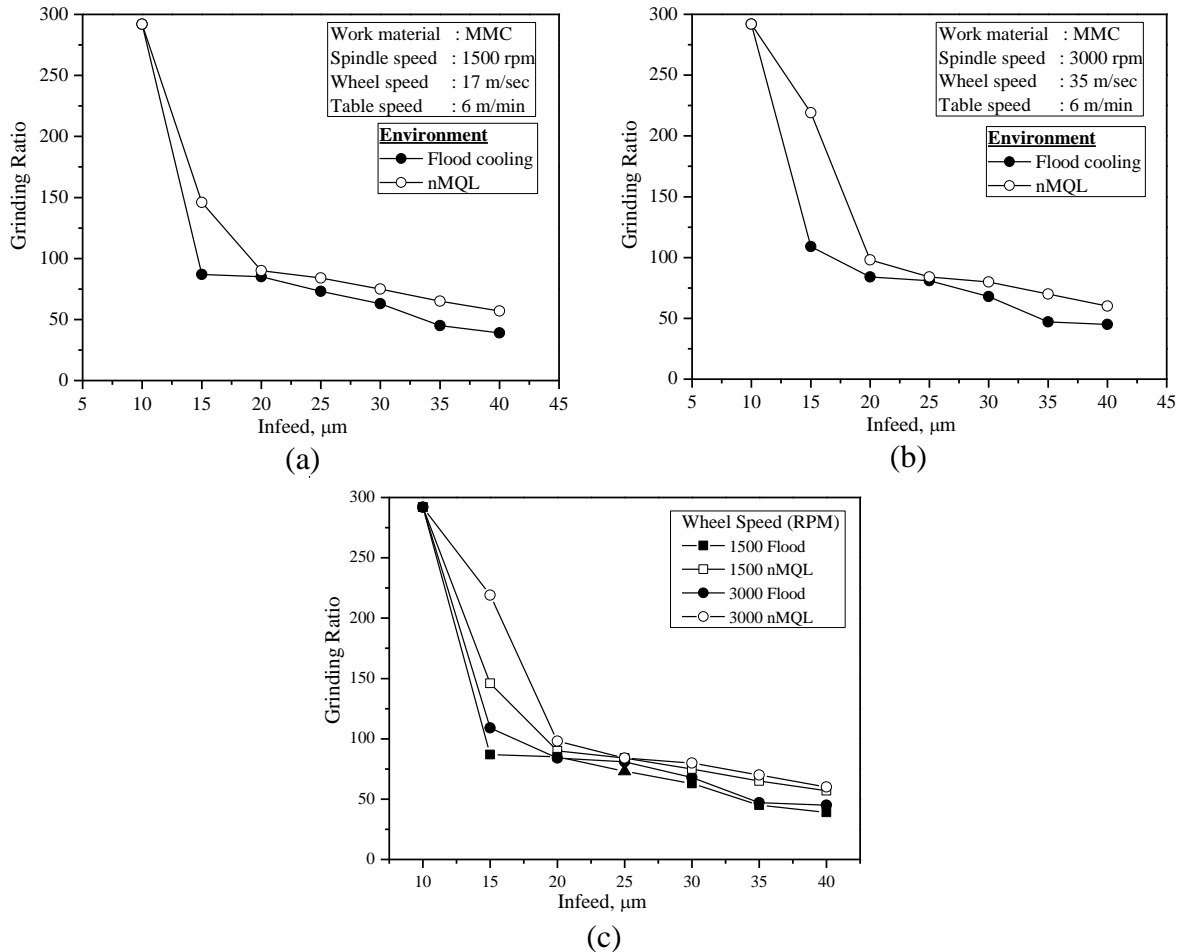

Fig. 2.17 Variation of grinding ratio with infeed under flood and nMQL conditions for (a) 1500 rpm (b) 3000 rpm, and (c) 1500 and 3000 rpm spindle speed

Fig. 2.17 illustrates that the grinding ratio decreases as the infeed increases and/or spindle speed decreases. This is because increased infeed or decreased spindle speed results in increased wheel wear, and the grinding ratio is the ratio of material removal from the workpiece to wheel wear. It lowers rapidly at the start because of very small amount of wheel wear at lower infeeds, but the rate of decline slows significantly in the latter portion. Furthermore, nMQL has a higher grinding ratio than flood cooling meaning that nMQL shows better grindability than flood cooling in grinding AL/SiC MMC.

Chapter-3

Modeling and Optimization

3.1   Predictive modeling of surface roughness using ANN

Artificial neural networks (ANN) works in a similar way by which human brain processes information. ANN consists of layers and each of the layer have neuron(s). A general ANN structure consists of three layers; input, hidden, & output layer. Each of the neuron of the input layer can receive one input value. These input values are transferred to the neurons of the hidden layers and the neurons of the hidden layers are conncted to the neuron(s) of the output layer. The hidden layer has n number of neurons. These artificial neurons of different layers are connected to each other in order to determine the relation of inputs and outputs. Neuron is the computational unit of an ANN structure. Both the neurons and the connections between the neurons have values associated with them. The values of the connections are called weights. Weights indicate the importance of the values of the neurons to the neurons of the next layer. The output layer provides the value of the response.

Neural networks are of two types; feed-forward type and the recurrent type. In feed-forward network, signals move in only one direction. The direction is from input to output such that the output signal of a neuron is the input to the neurons of the next layer. On the other hand, recurrent type networks permit signals to move forward and/or backward. One advantage of Feed forward back propagation neural network is that it has simple structure and it can be used in non-linear applications (Karimi & Yousefi, 2012).

ANN uses training algorithm to predict the pattern inside the data. The training data should cover a wide range of variable levels rather than confined to a small range to get better prediction performance. Over-training of the training data leads to poor prediction of new data. Addition of neurons improves the training performance. On the other hand, optimum performance of the testing data is observed with optimum number of

neurons (Karimi & Yousefi, 2012). The network was trained using the Levenberg–Marquardt algorithm (trainlm) as it can quickly train a moderate-size feed forward network. Moreover, it allows training with validation (Mia & Dhar, 2016). The trained ANN network is employed to predict testing data that was not included in the training data. The result of prediction is then compared with the experimental results. ANN provides impressive results in predicting non-linear data sets. A trained & tested ANN model can be used by providing input values to predict the response.

One way to improve ANN performance is to introduce more input levels. Greater input level creates larger experimental runs which is costly and time-consuming. However, there are other ways to alter ANN performance such as changing the number of hidden neurons and/or learning factors (J. P. Davim et al., 2008).The ANN structure used in this study was 2-n-1. Spindle speed and infeed were the two input neurons whereas surface roughness was the output neuron. n is the number of neuron(s) in the hidden layer(s). The value of n was chosen as 1-10,15,20,25, and 30 in this study. There is no standard method to determine the number of hidden layers and neurons in the hidden layers. Therefore, trial and error approach is adopted to determine the optimum number of layers as well as neurons.

A neural network may have multiple hidden layers or no hidden layers at all. Hidden layers are employed to increase the network performance. However, there is no clear theoretical benefit to using more than two hidden layers in neural networks. The use of two hidden layers in a neural network can present certain challenges. One issue is that the presence of additional layers may worsen the problem of local minima. To mitigate this, it is important to utilize various methods to obtain global optimization. Another challenge is that the additional hidden layer can make the gradient of the network more unstable, potentially slowing down the training process. In light of these considerations, it is often recommended to begin with a single hidden layer and, if necessary, increase the number of hidden neurons within that layer before adding additional layers. If a single hidden layer with a large number of neurons does not sufficiently improve performance, it may be worth considering the addition of a second hidden layer (Svozil et al., 1997). However, a single hidden layer was used in this study as it provided satisfactory results.

Previous studies found that tansig and logsig transfer functions provided similar results and logsig was frequently applied by researchers (Zain et al., 2010). Logsig was chosen in this study to be the transfer function. Table 3.1 lists the network properties that were employed in this study. Data from the 14 experimental runs with flood cooling environment were utilized where 70% of the data were used for training and the rest (30%) for testing. For each value of n mentioned earlier, three different sets of predicted values were recorded by running the model several times. From each of the set, one MSE value was calculated & averaged and are listed in Table 3.2.

Table 3.1 Network properties adopted in ANN

Category	Type
Network type	Feed forward back propagation
Training function	TRAINLM
Adaption learning function	LEARNGDM
Performance function	MSE
Number of layer	1
Number of neurons	1-10,15, 20, 25, & 30
Transfer function	LOGSIG

Four data sets are maintained separate in order to test the model. Best validation performance obtained in training period in terms of mean squared error are presented in Fig. 3.1 for flood cooling. The green line shows the validation error whereas the blue line shows the training error. The minimum amount of validation error is observed at epoch 0, as indicated by a green circle. The network parameters were recorded by the NN toolbox in matlab 2015. It is to be noted that the validation error curve does not necessarily decrease with each iteration; in fact, it may increase before decreasing to a lower value (Hagan et al., 1995). In addition, as shown in Fig. 3.2, the dotted line represents indistinguishable actual & predicted values whereas the solid line represents fit. A scatter plot of network outputs versus targets is a critical tool for network validation in function approximation problems. Here, Y axis represents the predicted value of surface roughness whereas X- axis represents the actual value of the surface roughness. The value of the correlation coefficient R using ANN is more than 99% indicating high correlation. During training, highest values of correlation coefficient (R) is found 0.99688 for one hidden layer and 9 neurons in the hidden layer (2-9-1). Average MSE values were also found lowest for that network structure. Fig. 3.3 shows predicted values and actual values of surface

roughness to provide model validation. MAPE of roughness was 1.23%, 1.17%, & 0.66% using ANN for first, second, & third trial respectively.
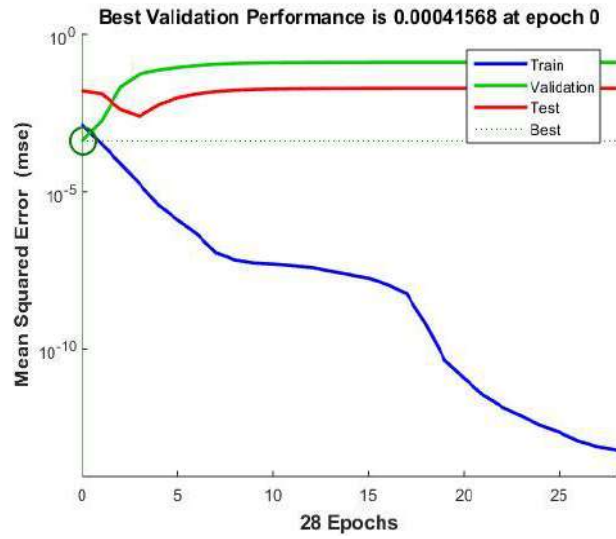
Fig. 3.1 Neural Network Training Performance based on MSE for flood cooling
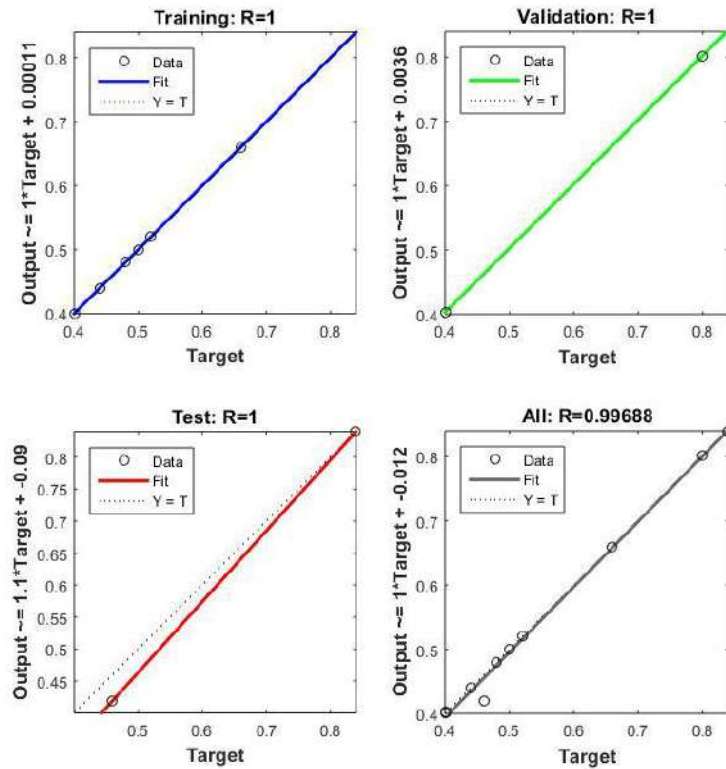
Fig. 3.2 Neural network correlation coefficient values at 2-9-1 structure

44

Table 3.2 MSE values for different network configurations

Network Structure	Trainlm, Learngdm, Logsig, No. of layer =1			
	1st trial	2nd trial	3rd trial	Average
2-1-1	0.00745	0.00097	0.00199	0.00347
2-2-1	0.05030	0.01622	0.00040	0.02231
2-3-1	0.01909	0.00322	0.00024	0.00752
2-4-1	0.00604	0.00198	0.00080	0.00294
2-5-1	0.00165	0.00252	0.00195	0.00204
2-6-1	0.00670	0.00226	0.01089	0.00662
2-7-1	0.00017	0.00077	0.00476	0.00190
2-8-1	0.00223	0.00328	0.00155	0.00235
2-9-1	0.00051	0.00078	0.00057	0.00062
2-10-1	0.00992	0.01131	0.00441	0.00854
2-15-1	0.00922	0.00851	0.00624	0.00799
2-20-1	0.00134	0.01304	0.01497	0.00978
2-25-1	0.00109	0.00935	0.00794	0.00613
2-30-1	0.00349	0.01254	0.01293	0.00966
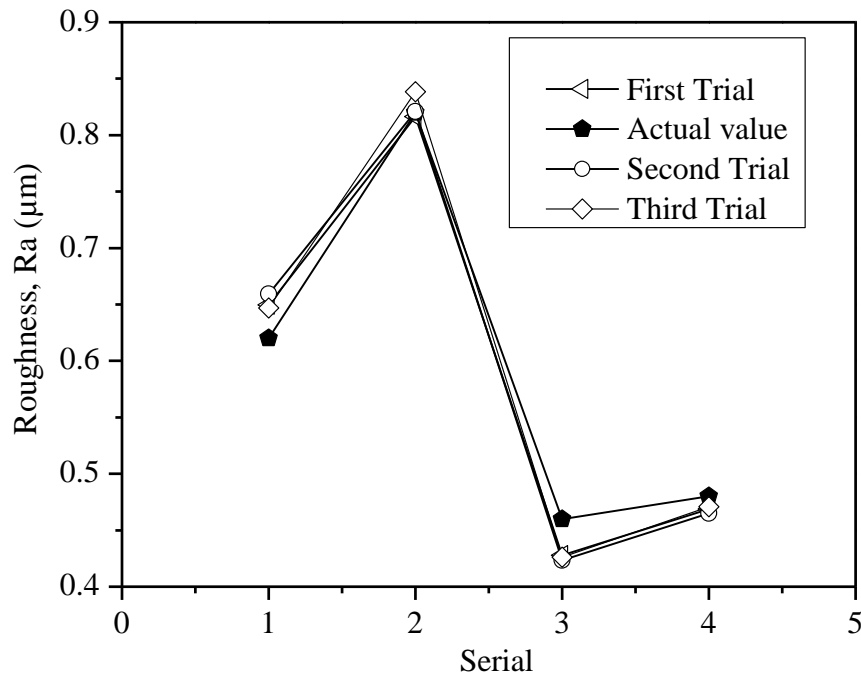
Fig. 3.3 Comparison between Actual and predicted values using 2-9-1 structure

3.2   Optimization of process parameters selection

Setting up of optimum machining parameters has been a great concern for manufacturing industries for more than a century where economy of machining operation plays a major role in competitiveness in the market (Tolouei-Rad & Bidhendi, 1997). Besides, machining process outputs depend upon cutting conditions. In addition, establishment of optimum cutting conditions have a great influence on production rate, operation cost, and product quality (Wang, 1993). Although the desirable cutting conditions for roughing can be obtained based on experience or handbook data, it does not ensure optimal or near optimal data for that particular machine setting and environment. To determine the optimal cutting conditions, reliable mathematical models need to be established between process inputs (factors) and outputs (responses) (Chua et al., 1993). Mathematical models are usually of two types; theoratical and empirical (Box & Draper, 1987). In many cases, the theoratical model that establishes a relation between controllable variables (factors) and a response either is not available or is very complex. Therefore, the relation between factors and response should be obtained in an empirical way (Sarabia & Ortiz, 2009). Empirical models are formulated based on experimental data. In order to ensure the effectiveness of the models, design of experiment technique should be used to plan the machining experiments efficiently. After that, the analysis of variance will then be applied to check the adequacy of each mathematical model and their respective parameters (Chua et al., 1993). In a nutshell, optimization process involves three major steps; conducting the designed experiments, estimating the coefficients in a mathematical model, predicting the response & checking the adequacy of the model (Sadhukhan et al., 2016).

Response surface methodology is a mathematical and statistical tool which is commonly used to model & optimize processes, and evaluates the relationship between factors (output variables) and responses (input variables).RSM is one of the most used methods for optimization in the last few years (Baş et al., 2007) and was introduced by Box and Wilson (Sarabia & Ortiz, 2009). This method is helpful in carrying out the analysis of experiments with very less experimental efforts (Raj & Senthilvelan, 2015). When the response can be defined by a linear function of independent variables, then the approximating function is called a first-order model. A first-order model having two independent variables can be expressed as below.

$y = \beta_0 + \beta_1 x_1 + \beta_2 x_2 + \varepsilon$ ....(3.1)

When there is a curvature in the response surface, then a higher degree polynomial should be used. The approximating function having two variables is called a second-order model and can be expressed in the format below.

$y = \beta_0 + \beta_1 x_1 + \beta_2 x_2 + \beta_{11} x^2_{11} + \beta_{22} x_{222} + \beta_{12} x_1 x_2 + \varepsilon$ ....(3.2)

Here, x_1 and x_2 are independent variables where the response y depends on them. The dependent variable y is a function of x_1 and x_2. The experimental error, denoted as **ε,** represents any measurement error on the response y, as well as other type of variations not counted by the model. The two most commonly used response surface modeling designs are central composite designs (CCD) and Box–Behnken designs (BBD). Here, the inputs take on three or five distinct levels, but all combinations of these values do not appear in the design. CCD can construct a second-order model efficiently (Montgomery, 1997). CCD is the most popular of the many classes of RSM. It is alsovery flexible, efficient, and provides much information on experimentalvariable effects & the overall experimental errors in a minimum number of required runs (Rahman & Kadirgama, 2014). CCD is a factorial or fractional factorial design. Here, center points are augmented with a group of axial (star) points which permits curvature shaped estimation. CCD contains cube points at the corners of a unit cube, center points at the origin, and star points along the axes at or outside the cube. A central composite design usually comprises twice the number of star points as the number of factors. New extreme values for each factor are represented by the star points. Ultimately, the placement of the star points determines the type of CCD. The star points are spaced at some distance α from the center according to the design features sought and the amount of factors in the design. The α values vary according on the number of factors included in the factorial section of the design. Face-centered central composite designs occur when the star points are located in the center of each face, where α is equal to one (Hanrahan et al., 2005). CCD has been applied in this research work by taking alpha value to 1.414 to design the experiments. Factors that are used along with their levels are listed in Table 3.3.

Table 3.3 List of factors with corresponding levels

Serial	Factor	Type	Unit	Level values	
1	Spindle speed	Continuous	r.p.m.	1500	3000
2	Infeed	Continuous	μm	15	35
3	Environment	Categorical	-	Flood	nMQL

A total of 26 experimental runs are obtained from this design using "Minitab version 17" statistical software. After that, experimental runs are performed and data are collected for four responses: tool wear, grinding ratio, grinding temperature, and surface roughness. CCD experimental design with response values and run order are listed in Table 3.4. After putting the data in minitab software, it automatically generates empirical modeling, main effects plot, interaction plot, and response optimizer for all of the four responses. The predictive models are given below.

$$G_{Flood} = 52.7 + 0.0976 \times N_s - 4.42 \times d - 0.000013 \times N_s \times N_s + 0.0856 \times d^2 - 0.001267 \times N_s \times d \quad ....(3.3)$$

$$G_{nMQL} = 71.4 + 0.0976 \times N_s - 4.42 \times d - 0.000013 \times N_s \times N_s + 0.0856 \times d^2 - 0.001267 \times N_s \times d \quad ....(3.4)$$

$$WW_{Flood} = 0.444 - 0.000567 \times N_s + 0.0093 \times d + 0.001325 \times d^2 \quad ....(3.5)$$

$$WW_{nMQL} = 1.040 - 0.000567 \times N_s - 0.0254 \times d + 0.001325 \times d^2 \quad ....(3.6)$$

$$R_{Flood} = 0.3308 + 0.000013 \times N_s + 0.01430 \times d + 0.000166 \times d^2 - 0.000005 \times N_s \times d \quad ....(3.7)$$

$$R_{nMQL} = 0.1283 + 0.000064 \times N_s + 0.01149 \times d + 0.000166 \times d^2 - 0.000005 \times N_s \times d \quad ....(3.8)$$

$$T_{Flood} = -176 + 0.0815 \times N_s + 80.16 \times d - 1.0595 \times d^2 \quad ....(3.9)$$

$$T_{nMQL} = -257.8 + 0.0418 \times N_s + 74.7 \times d - 1.0595 \times d^2 \quad ....(3.10)$$

ANOVA for the temperature surface roughness, wheel wear, and grinding ratio are presented in Table 3.5 to 3.8. Backward elimination of terms was applied to remove insignificant terms where $\alpha = 0.1$ was used. This means that any variable term having a p value greater than the α value will be removed from the model. The influence and percent contribution of each of the term has been calculated on the rightmost column of these tables. Infeed, cooling environment, infeed, & infeed are the most contributed factors with 53.4%, 40.402%, 77.259%, and 67% contributions respectively on the temperature, roughness, wheel wear, & Grinding ratio, respectively. The R^2 value and R^2 (adj) values

for the temperature, surface roughness, wheel wear, & grinding ratio are 99.36% & 99.16%, 96.35% & 94.93%, 95.11% & 93.56%, and 92.42% & 90.02%, respectively. These values are so much close to each other that is preferable. R^2 (adj) value of 99.36% implies that 99.36% of the total variation of the respective response can be described by the respective model. A higher R^2 value indicates the model better fits the data. Based on these values we can conclude that these models are highly acceptable. Model F is the ratio of the individual term mean square value to the residual mean square value. F values for the responses are 494.19, 67.91, 61.54, and 38.6, respectively. Therefore, it can be claimed that the models are significant.

Table 3.4 Central composite design along with response values

Run Order	Spindle Speed (rpm)	Infeed (μm)	Environment	Wear (mm³)	G ratio	Roughness (μm)	Temperature (℃)
1	3000	35	MQL	1.09956	73.211	0.42	1171
2	3310	25	Flood	0.78540	73.211	0.44	1450
3	2250	25	MQL	0.62832	91.514	0.38	1030
4	1200	25	MQL	0.78540	73.211	0.46	970
5	2250	10	MQL	0.07854	292.844	0.28	560
6	2250	25	Flood	0.70686	81.346	0.54	1372
7	1500	35	MQL	0.86394	93.178	0.50	1130
8	2250	40	MQL	1.33518	67.427	0.58	1180
9	2250	25	MQL	0.62832	91.514	0.38	1030
10	1500	15	MQL	0.31416	109.817	0.36	700
11	2250	25	Flood	0.70686	81.346	0.54	1372
12	3000	15	Flood	0.23562	146.422	0.44	990
13	1200	25	Flood	1.02102	56.316	0.66	1260
14	2250	10	Flood	0.07854	292.844	0.38	740
15	2250	25	Flood	0.70686	81.346	0.54	1372
16	2250	25	Flood	0.70686	81.346	0.54	1372
17	3000	15	MQL	0.15708	219.633	0.30	740
18	2250	25	Flood	0.70686	81.346	0.54	1372
19	2250	25	MQL	0.62832	91.514	0.38	1030
20	3300	25	MQL	0.70686	81.346	0.30	1090
21	2250	25	MQL	0.62832	91.514	0.38	1030
22	2250	40	Flood	2.35620	38.209	0.74	1500
23	1500	15	Flood	0.47124	73.211	0.48	900
24	1500	35	Flood	1.80642	44.563	0.82	1430
25	3000	35	Flood	1.72788	46.589	0.50	1560
26	2250	25	MQL	0.62832	91.514	0.38	1030

Table 3.5 ANOVA for the grinding zone temperature

Source	DF	Adj. SS	Adj. MS	F- Value	P- Value	% Contribution
Model	6	1780393	296732	494.19	0.000	99.36
Linear	3	1606032	535344	891.59	0.000	89.63
N_s	1	34170	34170	56.91	0.000	1.91
d	1	956785	956785	1593.48	0.000	53.40
Environment	1	615077	615077	1024.38	0.000	34.33
Square	1	158886	158886	264.62	0.000	8.87
d×d	1	158886	158886	264.62	0.000	8.87
2-Way Interaction	2	15475	7738	12.89	0.000	0.86
$N_s \times$ Environment	1	3540	3540	5.90	0.025	0.20
d ×Environment	1	11935	11935	19.88	0.000	0.67
Error	19	11408	600	-	-	0.64
Lack-of-Fit	9	11408	1137	-	-	0.64
Pure Error	8	0	0	-	-	0.00
Total	25	179180	-	-	-	100.00
Model Summary	S=24.504, R^2 = 99.36%, R^2 (adj)= 99.16%, R^2 (pred)= 98.47%					

Table 3.6 ANOVA for the Surface roughness

Source	DF	Adj. SS	Adj. MS	F- Value	P- Value	% Contribution
Model	7	0.413290	0.059041	67.91	0.000	96.35
Linear	3	0.389157	0.129719	149.21	0.000	90.73
N_s	1	0.067263	0.067263	77.37	0.000	15.68
d	1	0.158679	0.158679	182.52	0.000	36.99
Environment	1	0.163215	0.163215	187.74	0.000	38.05
Square	1	0.003915	0.003915	4.50	0.048	0.91
d×d	1	0.003915	0.003915	4.50	0.048	0.91
2-Way Interaction	3	0.020218	0.006739	7.75	0.002	4.71
$N_s \times$ d	1	0.011250	0.011250	12.94	0.002	2.62
$N_s \times$ Environment	1	0.005808	0.005808	6.68	0.019	1.35
d ×Environment	1	0.003160	0.003160	3.63	0.073	0.74
Error	18	0.015649	0.000869	-	-	3.65
Lack-of-Fit	10	0.015649	0.001565	-	-	3.65
Pure Error	8	0.00000	0.000000	-	-	0.00
Total	25	0.428938	-	-	-	100.00
Model Summary	S=0.0295, R^2 = 96.35%, R^2 (adj)= 94.93%, R^2 (pred)= 87.59%					

Table 3.7 ANOVA for the wheel wear (WW)

Source	DF	Adj. SS	Adj. MS	F- Value	P- Value	% Contribution
Model	8	6.69360	1.11560	61.54	0.000	95.11
Linear	3	5.93584	1.97861	109.14	0.000	84.34
N_s	1	0.02889	0.02889	1.59	0.222	0.41
d	1	5.42652	5.42652	299.32	0.000	77.10
Environment	1	0.48043	0.48043	26.50	0.000	6.83
Square	2	0.27503	0.13752	7.59	0.004	3.91
$N_s \times N_s$	1	0.05666	0.05666	3.13	0.093	0.81
d×d	1	0.24439	0.24439	13.48	0.002	3.47
2-Way Interaction	1	0.48272	0.48272	26.63	0.000	6.86
d ×Environment	1	0.48272	0.48272	26.63	0.000	6.86
Error	19	0.34446	0.01813	-	-	4.89
Lack-of-Fit	11	0.34446	0.03131	-	-	4.89
Pure Error	8	0.00000	0.00000	-	-	0.00
Total	25	7.03806	-	-	-	100.00
Model Summary	S=0.1346, R^2=95.11%, R^2 (adj)= 93.56%, and R^2 (pred)= 89.25%

Table 3.8 ANOVA for the grinding ratio (G)

Source	DF	Adj. SS	Adj. MS	F- Value	P- Value	% Contribution
Model	6	19718.5	3286.4	38.60	0.000	92.42
Linear	3	16940.7	5646.9	66.33	0.000	79.40
N_s	1	374.0	374.0	4.39	0.050	1.75
d	1	14295.6	14295.6	167.92	0.000	67.00
Environment	1	2271.1	2271.1	26.68	0.000	10.64
Square	2	2055.8	1027.9	12.07	0.000	9.64
$N_s \times N_s$	1	769.6	769.6	9.04	0.007	3.61
d×d	1	1020.1	1020.1	11.98	0.003	4.78
2-Way Interaction	1	722	722	8.48	0.009	3.38
$N_s \times d$	1	722	722	8.48	0.009	3.38
Error	19	1617.5	85.1	-	-	7.58
Lack-of-Fit	11	1617.5	147.0	-	-	7.58
Pure Error	8	0.00000	0.00000	-	-	0.00
Total	25	21336.0	-	-	-	100.00
Model Summary	S=9.2268, R^2 =92.42%, R^2 (adj)= 90.02%, and R^2 (pred)= 82.71%

Using the equations 3.3 to 3.10, predicted values for the settings listed in Table 3.8 has been calculated and compared with the measured value for validation purposes. MAPE values are found to be 4.3% & 5.22%, 2.64% & 0.69%, 3.01% & 6.8%, 8.67% & 8.58% for the T_{Flood} & T_{nMQL}, R_{Flood} & R_{nMQL}, WW_{Flood} & WW_{nMQL}, G_{Flood} & G_{nMQL}, respectively. The comparison of measured and predicted values are shown in Fig. 3.4 and Fig. 3.5. The figure shows that the measured and predicted values are very close to each other. So it can
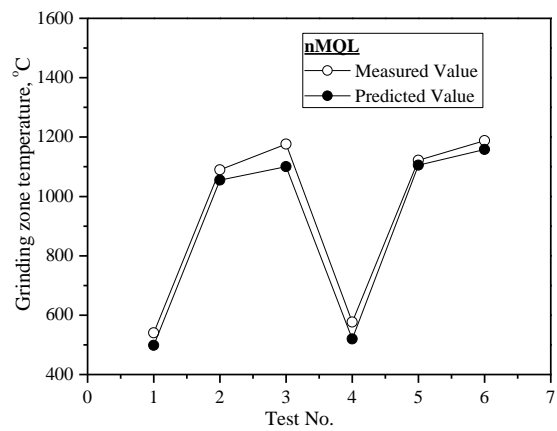
be claimed that the models are acceptable for predicting the responses from process parameters.

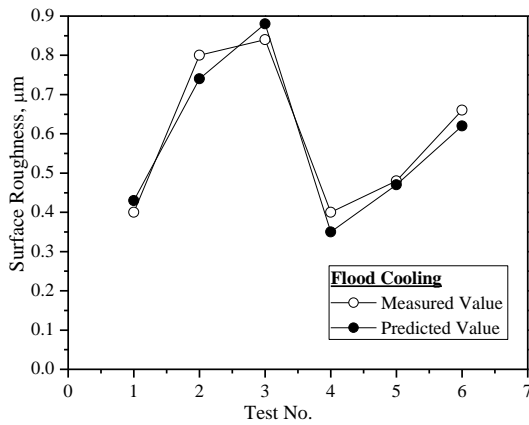**Table 3.9** Parameter settings for validity test

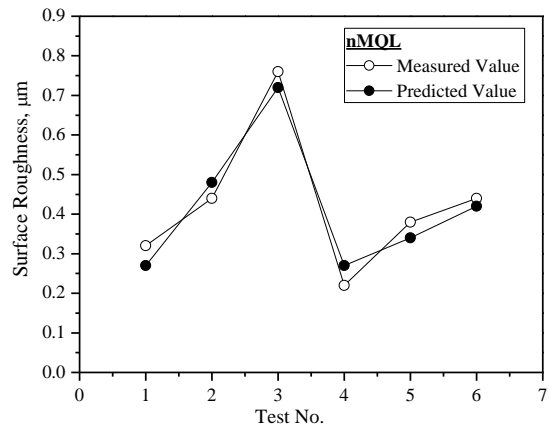| Test Number	Spindle Speed	Infeed
1	1500	10
2	1500	30
3	1500	40
4	3000	10
5	3000	30
6	3000	40
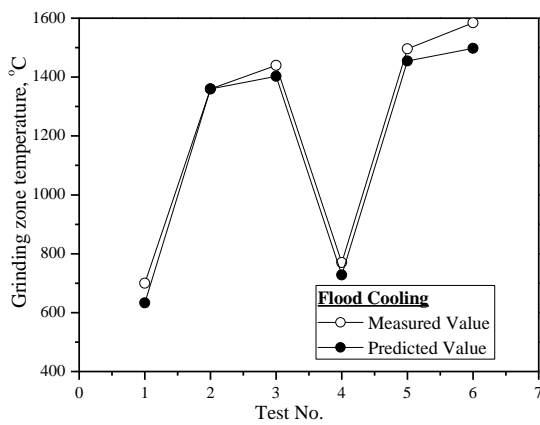
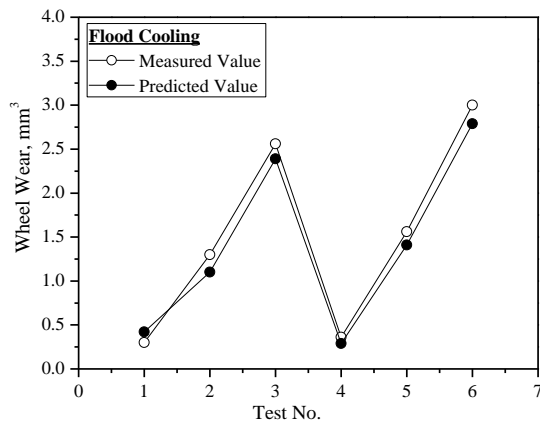(a) Temperature, Flood Cooling

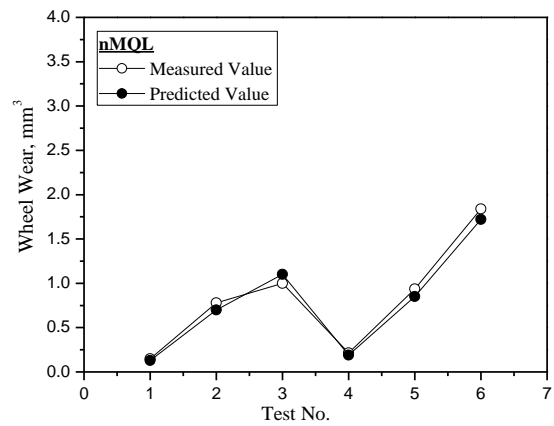(a) Temperature, nMQL

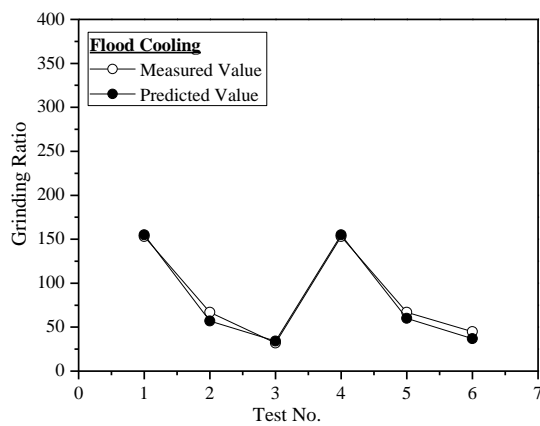(a) Roughness, Flood Cooling

(a) Roughness, nMQL

Fig. 3.4 Validation of predicted values with measured values for temperature & roughness while grinding Al/SicMMC under flood and nMQL conditions
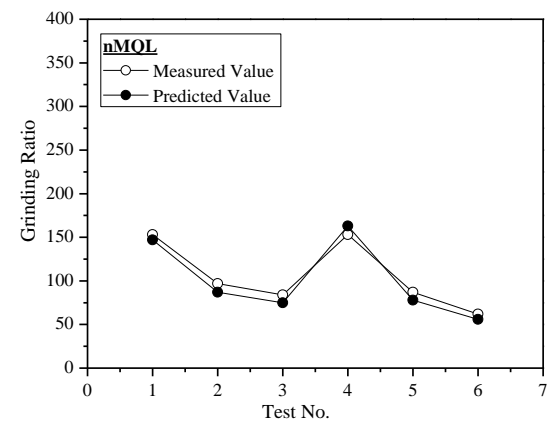
Fig. 3.5 Validation of predicted values with measured values for wheel wear and grinding ratio while grinding Al/SicMMC under flood and nMQL conditions

The residual plots for each of the responses are presented in Fig. 3.6. From the figure, we can see that most of the points are along the straight line in the normal probability plot. The histograms are likely to be normally distributed for the residual values. Since the residual plots represent both the flood and nMQL conditions for a single response, histograms may contain double normally distributed plots (Fig. 3.6 (a)). For the residual versus fitted value plot, the residual values are random and fairly above and below the zero residual line. In case of the residual versus observation order plot, no clear trends or pattern can be identified and the residuals are found to be random around the centerline. Therefore, it can be concluded that the effect of experiment order on the residual values is insignificant.

(a) Temperature   (b) Surface roughness

(c) Wheel Wear   (d) Grinding Ratio
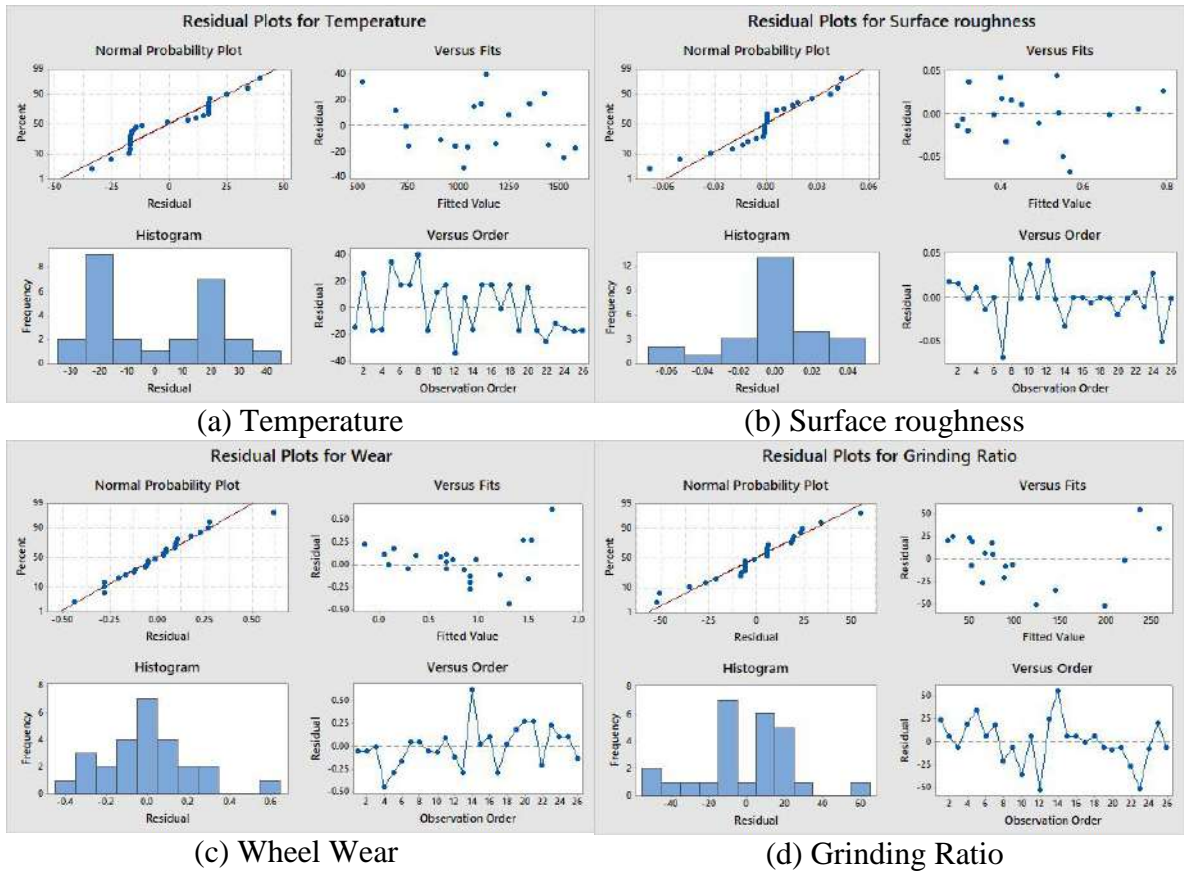
Fig. 3.6 Residual Plots for different responses

Main effect plot shows the relationship between individual factors with the response. On the other hand, Interaction plot provides the combined effect of the factors on output response (H. Tusar, 2019). Fig. 3.7 to 3.10 provides the main effect and interaction plot for grinding zone temperature, surface roughness, and tool wear, respectively. It can be claimed based on the main effect plot for temperature (Fig. 3.5) that higher spindle speed produces greater amount of temperatures though the rate of increase of temperature is low. On the other hand, higher infeed created greater temperatures, largely at the begining and then relatively slowly. Infeed values showed significant amount of effect on temperature values. Besides, nMQL produced significantly lower temperature than the flood cooling. Fig. 3.7 also shows the interaction effects of spindle speed with infeed and cooling environment. With the increase of spindle speed, temperature increased differently for the infeed and the environment. The rate of temperature increase for flood cooling is comparatively greater than nMQL with the increase of speed. The rate of temperature increase with lower infeeds is comparatively slower than higher infeeds with the rise of

spindle speed. With the increase of infeed, rate of increase of temperature is greater for flood cooling than nMQL.
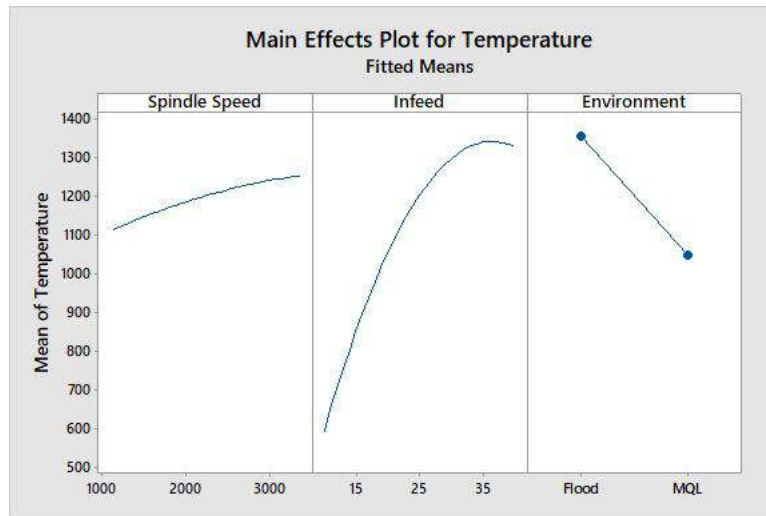
(a)
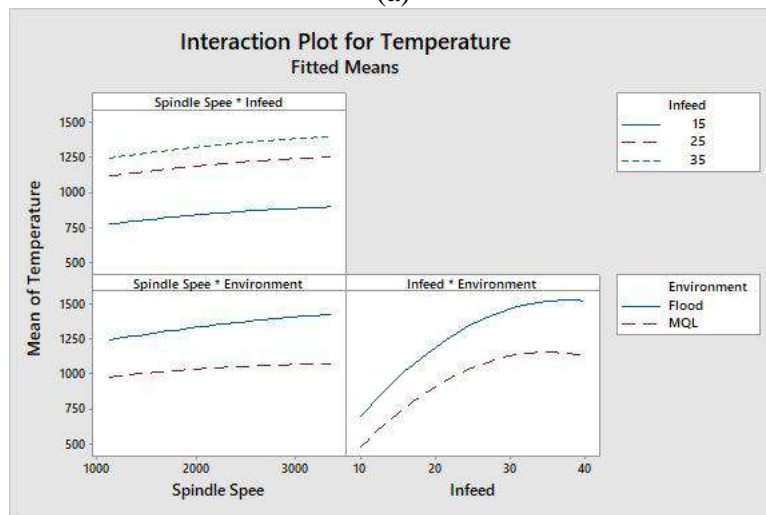
(b)

Fig. 3.7 (a) Main effects plot and (b) Interaction plot for the temperature

As shown in Fig. 3.8, for surface roughness (R), higher values of spindle speed and lower values of infeed provides better surface finish. Roughness reduces linearly with increasing spindle speed whereas roughness increases sharply at higher infeeds. On the other hand, nMQL produces better surface than flood cooling. From Fig. 3.8, it is seen that all of the three combined effects have significant impact on surface roughness. The rate of reduction of surface roughness with the increase of spindle speed is slower for lower infeeds. The rate of reduction of surface roughness with the increase of spindle speed is slower for the nMQL approach than flood cooling. The rate of roughness increase with infeeds with slightly greater for flood cooling than nMQL.
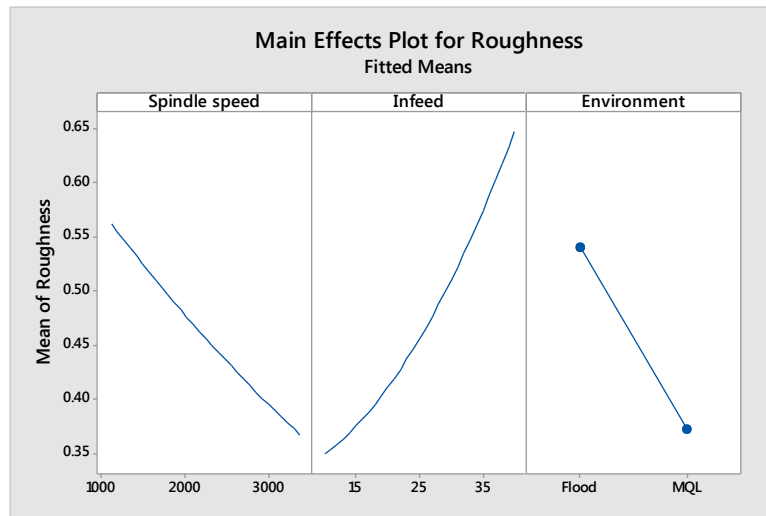
(a)
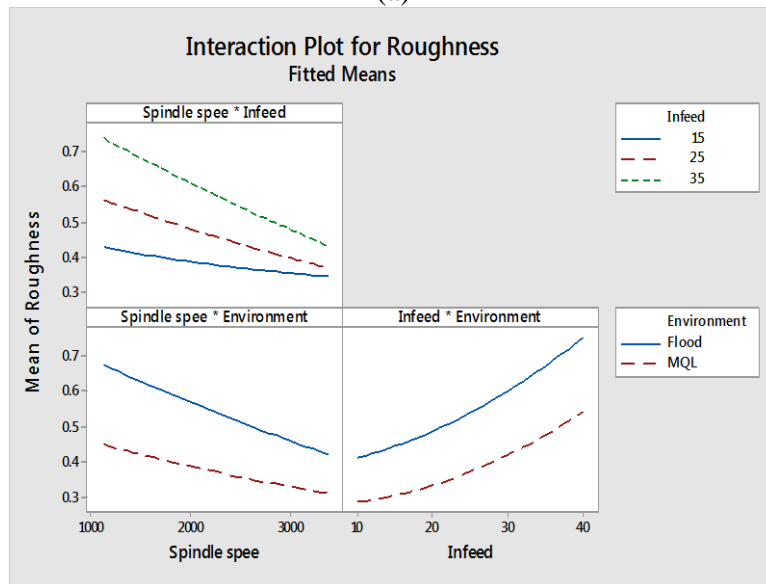
(b)

Fig. 3.8 (a) Main effects plot and (b) Interaction plot for the surface roughness

It can be shown from the main effect plot shown in Fig. 3.9 that the rate of reduction in wheel wear is slow with the increase of spindle speed. Increased infeed results in increased wheel wear. It increases gradually at first, then rapidly in the latter section. nMQL caused less wear than flood cooling, as can be seen clearly in the image. From the interaction plot for tool wear, it is observed that the rate of wear reduction with increased spindle speed is lower for lower infeeds. Also, the rate of wear reduction with increased spindle speed is comparatively lower for the nMQL environment. On the other hand, the

56

rate of increase in wear with increased infeed is greater for the flood cooling than the nMQL.
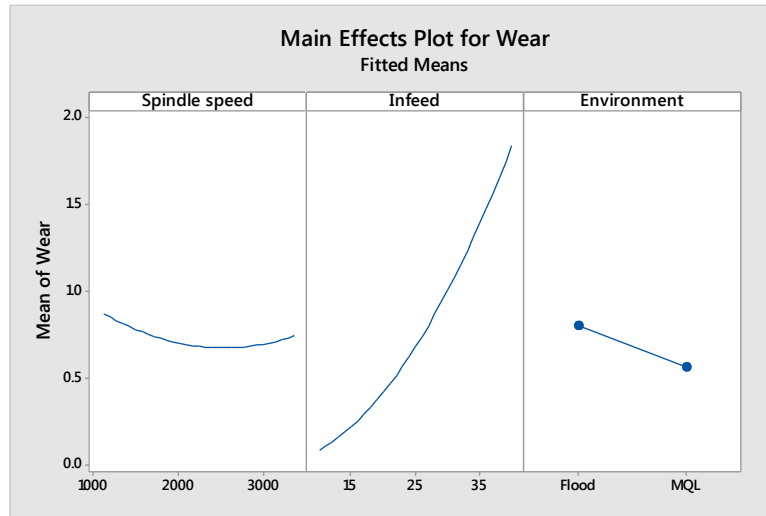
(a)
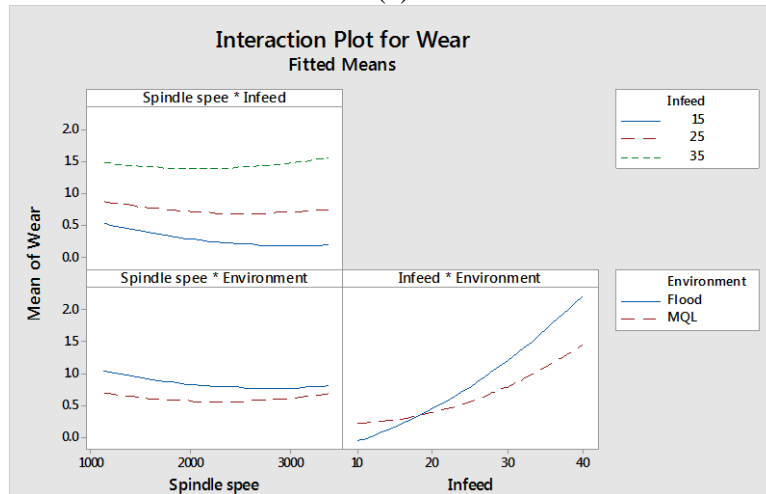
(b)

Fig. 3.9 (a) Main effects plot and (b) Interaction plot for the wheel wear

Fig. 3.10 presents main effects plot and interaction plots for the grinding ratio. The main effect plot shows that higher grinding ratio is associated with higher spindle speed and lower infeeds. It falls sharply at lower infeeds but the rate of reduction slows at higher infeed values. nMQL produced higher grinding ratio than flood cooling. The interaction plot indicates that lower infeeds increase grinding ratio more effectively compared to higher infeeds with the increase of the spindle speed. Since the lines are parallel, spindle speed*environment and infeed*environment plots indicate no interaction effect. That means, with the increase of spindle speed, the rate of increase of grinding ratio is same

57

both for nMQL and flood cooling. Besides, the effectiveness of nMQL and flood cooling are same in reducing grinding ratio with respect to infeeds.
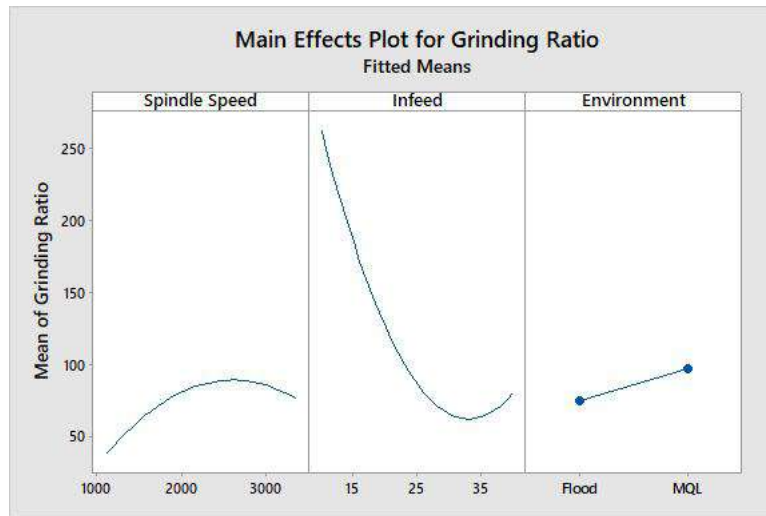
(a)
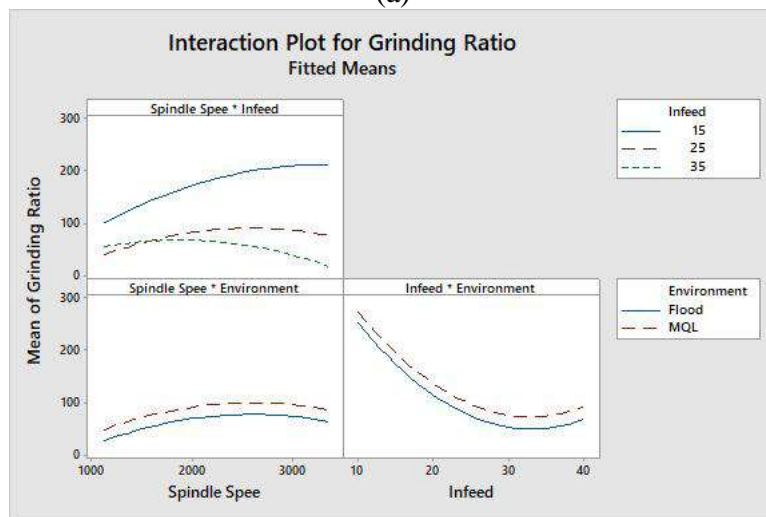
(b)

Fig. 3.10 (a) Main effects plot and (b) Interaction plot for the grinding ratio

To get the optimum values of input parameters for different environment and tool-work combinations, optimization needs to be carried out for single and multi-objective scenarios. Here, optimization has been carried out using "Minitab version 17" statistical software. Inside the minitab software, "RSM response optimizer" tab is selected first. One of the four goals must be chosen for each of the responses. These goals are minimize, minimize, maximize, and minimize for temperature, surface roughness, grinding ratio, and wheel wear, respectively. The weight and importance values for all the responses are set to the default value 1 to ensure equal relative importance for all the responses. Optimizing four responses concurrently for all environment provides the optimum parameters as

58

follows: spindle speed 2968 ~3000 r.p.m., infeed 10 μm, and environment nMQL. The value of composite desirability is 0.9783 which is very close to one indicating favorable results for the corresponding responses against the optimum setting. The desirability value could be zero to one. The optimum parameters obtained considering four responses are presented in Fig. 3.11.
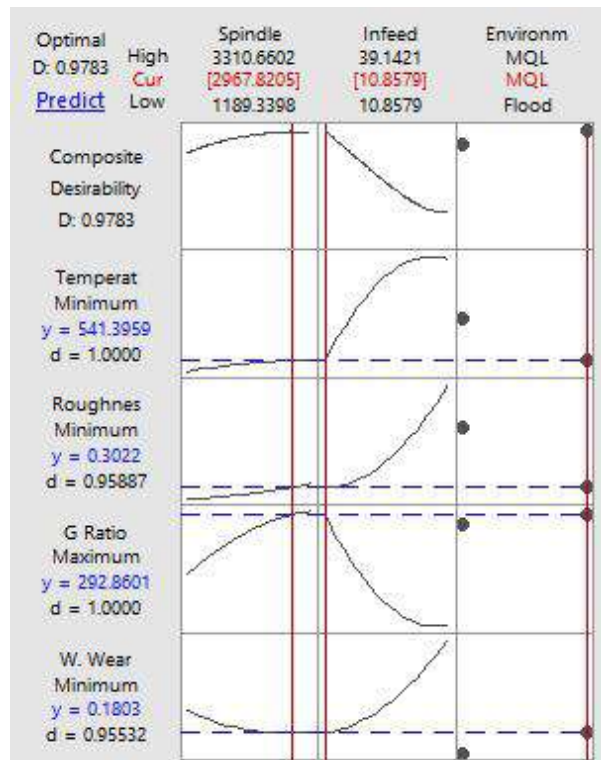
Fig. 3.11 Optimization using RSM based desirability function

Chapter-4

Discussions on Experimental Results

4.1   Chips morphology

The lower surface of the chips becomes immensely hot as it directly contacts the wheel. On the other hand, the upper surface of the chip becomes less hot due to efficient cooling with nMQL. The huge temperature difference between the two opposite surfaces of the chip causes the chip to act as a bimetallic spring, thereby causing the chip to curl to a tiny radius, as shown in Fig. 4.1(a). Bigger chips might occur when the temperature difference between the two surfaces is not significant. Therefore, bigger chips were produced (slice type) during flood cooling because of ineffective cooling (Fig. 4.1(b)). However, bigger chips were generated with higher infeed values due to greater penetration (M. I. H. Tusar et al., 2022).
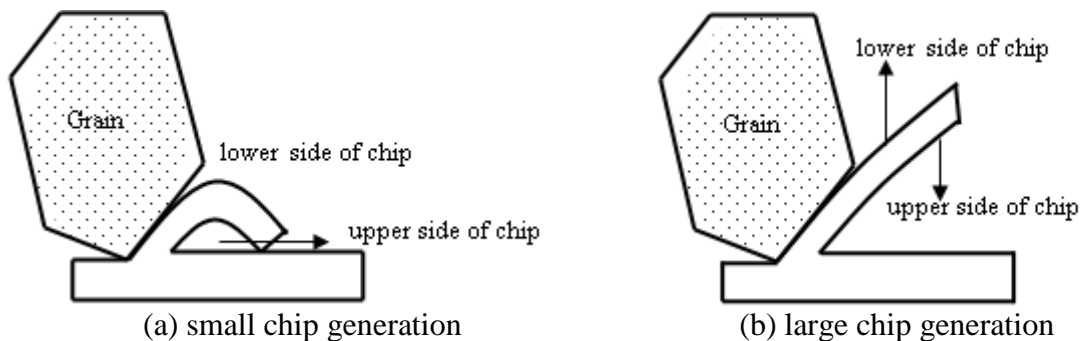
(a) small chip generation   (b) large chip generation
Fig. 4.1 Effect of temperature difference on chip size (Setti et al., 2015)

In this study, grinding chips are collected during each of the experimental run so that chips of different spindle speed, infeed, and environment combinations can be observed. Type of grinding wheel and workpiece material also have influences on the type of chips produced. Here, CBN grinding wheel is used to grind Aluminium based metal matrix composite. Chip morphology has been studied through visual observation and Scanning electron microscope (SEM) photos. Almost all of the chips are of slice, knife,

and shearing type. No chips are from ripping and melting type. Generation of slice chips frequently in flood cooling indicates greater wheel loading. On the other hand, nMQL approach produced insignificant amount of slice chips but mainly shearing & knife type chips indicating less wheel loading & efficient grinding. Low infeed values are suggested for less wheel loading.

4.2   Grinding zone temperature

Thermal conductivity, a parameter that indicates a material's ability to conduct heat, is critical for thermal analysis (Sinha et al., 2017). Thermal conductivity is critical for materials since the substrate frequently must dissipate huge amounts of heat, particularly in high-power devices. In this case, a high K value is desired to maintain low operating temperatures and minimize device failure due to overheating. Al-SiC MMC shows high thermal conductivity, usually between 200-220 W/m K (Davis & Artz, 1995). For grinding such a high thermally conductive material, flood cooling method is ineffective since only 4 to 30% of the applied fluid can reach the grinding zone, as discussed in the literature review. From Fig. 2.14, it is observed that flood cooling generates temperatures ranging between 700 to 1600°C for grinding the workpiece material. On the other hand, ZnO-deionized water based nMQL reduced the temperature to 500 to 1200°C, thereby 33.33% reduction in temperature for nMQL than flood cooling (for 3000 rpm spindle speed and 40 μm infeed). This may be because of the effective lubrication of nMQL method in reaching the grinding zone and enhanced thermal conductivity of the ZnO-deionized water nanofluid. 33% increase in thermal conductivity is reported after suspending ZnO NPs in water where the thermal conductivity of water and ZnO is 0.578 and 100 W/m-K respectively (Sinha et al., 2017). From literature it can be claimed that nMQL with water as base fluid can be superior to conventional flood coolant (Do Nascimento et al., 2016). Also, studies found that nMQL with water provides better cooling capacity than MQL without water, though with slightly lower lubricating capacity based on the grinding force result (Mao et al., 2012). Lubricaing property can be improved by adding nanoparticles in the water. Besides, pressurized air that instantly eliminates micro chips from the wheel pores, ensuring that the grits remain as sharp as possible and thereby reducing friction.

The dynamic viscosity of a fluid is a measure of its internal resistance to flow. It is obvious that when the concentration of NPs increases, the solution's dynamic viscosity

increases. This could be because a higher concentration of NPs causes more perturbation in the solution. The other straightforward alternative is that this results in an increase in the solution's density, which ultimately results in an increase in viscosity.The viscosity of the NFs increased approximately fourfold when compared to deionized water. Increased viscosity may aid in lubricating the contacting surfaces during actual grinding (Sinha et al., 2017).

It can be claimed based on the plot for temperature (Fig. 3.7) that increased spindle speed generates more heat, albeit the rate of growth is slow. Additionally, increased infeed results in increased temperatures, initially rapidly and then gradually. Without a doubt, it can be said the temperature of the grinding zone is impacted by process parameters, particularly the cutting environment.

4.3   Surface roughness

In this research work, surface grinding of Al-SiC metal matrix composite has been performed with a CBN grinding wheel at different spindle speed, infeed, and cooling environment. It is found from the main effect plot (Fig. 3.8) that higher values of spindle speed and lower values of infeed provides better surface finish. On the other hand, nMQL produces better surface than flood cooling.

In all cases, nMQL produced better surface roughness than that's of flood cooling method. This may be because of the enhanced cooling and lubrication system provided by the nMQL. Effective lubrication helps to slide the chips smoothly over the ground material. Therefore, less friction was created that helped to drop the roughness values. Moreover, compressed air in nMQL moves away the chips that results in lower wheel loading. ZnO nanoparticles are mixed with base fluid deionized water that are applied through nMQL along with compressed air. ZnO is well known for maintaining its cooling and lubricating properties at elevated temperatures. Besides, formation of tribo film produced from the nanofluid reduces tool wear and improves surface finish. Besides, the nanofluid contains deionized water and ZnO nanoparticles having significant thermal conductivity. The enhanced thermal conductivity of both the nanofluid and the CBN grinding wheel causes greater heat transfer from the grinding zone. As a result, tool wear and surface roughness are reduced.

Lower surface roughness values were observed in case of higher spindle speed. This might be because for higher spindle speed, greater number of abrasives participate in the cutting process. Higher roughness values were associated with higher infeeds. For higher infeeds, wheel grinds deep that results in more clogging of chips into the wheel surface. Therefore, higher surface roughness values were found.

4.4   Wheel wear

In this experiment, nMQL assisted grinding provided less wheel wear for every experimental compared to flood cooling. Thereby, nMQL is a better option than flood cooling in terms of wheel wear for any combination of spindle speed and infeed. Tool wear increased with the higher infeed both for flood cooling and nMQL. The rate of the rise is higher at higher infeed (35 and 40 μm) and lower at initial infeeds (10, 15, and 20 μm). However, less wear was noticed comparatively with 3000 rpm spindle speed compared to 1500 rpm. High grinding zone temperature results in localized diffusion and wheel loading. Due to lower heat generation with Zinc Oxide assisted grinding, wheel retains its cutting ability for a longer period of time. Besides, NF assisted grinding shows better cooling & lubricity due to formation of a stable tribo film. Moreover, nanofluids create a stable tribo-film that enables smooth sliding of the grains & easy shearing of the work material. In addition, nanofluids have viscosity sufficient enough to form an interface between the work and wheel surface generating hydrodynamic pressure that results in lower values of friction coefficient (Sinha et al., 2017). Therefore, nMQL assisted grinding created less coefficient of friction than wet grinding. Lower coefficient of friction results in reduced plastic deformation and less wheel wear.

4.5   Grinding ratio

Grinding ratio is the volume of metal removed in relation to the volume of wheel worn away (Krabacher, 1959). It is one of the measures to evaluate grindability (Inasaki &Nakayama, 1986). In addition, it is the most widely used parameter to evaluate the performance of grinding wheel (Kwak & Ha, 2002). It was reported that the grinding ratio falls as the metal removal rate increases and increases when the workpiece diameter, chip load, and grinding fluid concentration increase (Krabacher, 1959). From Fig.3.10, It is

observed that increased spindle speed increases the grinding ratio. Furthermore, as infeed increases, grinding ratio decreases. This is because a higher infeed causes more wheel wear, and the more the wheel wear, the lower the grinding ratio for equal amount of material removal. It begins with a fast drop, but the pace of decline slows as it progresses. When grinding is performed with nanofluids, formation of a slurry layer prevents wheel grain fracture. Hence, in this study, nMQL has a higher grinding ratio than flood cooling. Similar results were obtained by (Shen et al., 2008)

Chapter-5

Conclusions and Recommendations

5.1   Conclusions

Al/SiC MMC shows poor grindability due to clogging of the soft Al matrix and highly abrasive SiC reinforcement. The main purpose of this research is to design and develop an effective, efficient, and ecofriendly cutting fluid application system to enhance the grindability of Al-SiC MMC and to investigate its effects on chip, temperature, tool wear, grinding ratio, and surface roughness for getting optimal grinding parameters. The main contributions of this research work are as follows:

i)   A suitable grinding nozzle integrated with mixing chamber has been designed and fabricated to deliver continuous flow of nanofluids towards the grinding zone. Appropriate parameters for MQL set-up are found to be as follows: taper shaped nozzle, 13 mm inlet diameter of the nozzle, and 5 holes through which compressed air and nanofluid separately enter the mixing chamber.

ii)   An ecofriendly nanofluid of 0.5% concentration has been prepared and applied in grinding by suspending ZnO NPs and surfactant SDS in the DI water by ensuring uniform dispersion and proper stability of ZnO in the water to enhance the cooling and lubricating properties of the cutting fluid.

iii)   Effects of the prepared ecofriendly nanofluid through MQL on the grindability of Al-SiC MMC by CBN grinding wheel has been evaluated in respect of chip morphology, wheel wear, grinding ratio, temperature, and surface roughness. Significant reduction in clogging of workpiece material into the CBN grinding wheel is observed for both the flood cooling and nMQL compared to dry grinding. Application of the produced nanofluids through nMQL significantly improves the grindability of the material compared to conventional flood cooling method. While comparing between flood cooling and nMQL, less clogging is found for nMQL

than conventional flood cooling, thereby more efficient and economical approach for grinding Al/SiC MMC. Generation of slice chips frequently in flood cooling indicates greater wheel loading. On the other hand, nMQL approach produced insignificant amount of slice chips but mainly shearing & knife type chips indicating less wheel loading & efficient grinding. Low infeed values are suggested for less wheel loading.

iv) Compared to flood cooling, temperature, roughness, & wheel wear reduced about 25%, 42%, and 60% for nMQL approach. nMQL increased the grinding ratio by 60% compared to flood cooling. Infeed, cooling environment, infeed, & infeed are the most contributed factors with 53.4%, 40.402%, 77.259%, and 67% contributions respectively on the temperature, roughness, wheel wear, & Grinding ratio, respectively.

v) Based on the experimental data, empirical model for predicting surface roughness have been developed and validated using artificial neural network (ANN). MAPE of roughness using RSM was 1.67% whereas it was 1.23%, 1.17%, & 0.66% using ANN for first, second, & third trial respectively. Compared to RSM, better prediction was offered by ANN in predicting surface roughness.

vi) Spindle speed 3000 rpm, infeed 10 μm, and environment nMQL have been selected to be the desired optimal combination for enhancing the grindability of Al-SiC based MMC.

5.2   Recommendations

The following are some suggestions for future research:

i) Effects of nMQL with the same nanofluid in respect of cutting force and work surface are beyond the scope of this research. This could be a possible scope for future researchers in this field.

ii) Some other wheel could be involved to determine the suitable grinding wheel for grinding MMCs, i.e. diamond wheel, SiC wheel, Al_2O_3 wheel etc.

iii) Some other ecofriendly nanoparticles can be used in future for grinding through nMQL to investigate their effects on different responses, i.e. Ag nanoparticles.

References

Agarwal, S., "On the Mechanism and Mechanics of Wheel Loading in Grinding", Journal of Manufacturing Processes, Vol.41, PP.36-47, 2019.

Aurich, J. C., Herzenstiel, P., Sudermann, H., and Magg, T., "High-Performance Dry Grinding Using a Grinding Wheel with a Defined Grain Pattern", CIRP Annals - Manufacturing Technology, Vol.57(1), PP. 357-362, 2008.

Aurich, J., & Effgen, C., "Grinding", CIRP Encyclopedia of Production Engineering, PP. 586–589, 2014.

Bala, N., Saha, S., Chakraborty, M., Maiti, M., Das, S., Basu, R., & Nandy, P., "Green synthesis of zinc oxide nanoparticles using Hibiscus subdariffa leaf extract: effect of temperature on synthesis, anti-bacterial activity and anti-diabetic activity", RSC Advances, Vol.5(7), PP.4993–5003, 2014.

Baş, D., Ismail, H. B., "Modeling and optimization I: Usability of response surface methodology", Journal of Food Engineering, Vol.78(3), PP. 836-845, 2007.

Bianchi, E. C., Aguiar, P. R., Canarim, R. C., & Diniz, A. E., "Optimization of minimum quantity lubrication in grinding with CBN wheels", Machining and Machine-Tools, PP. 113–133, 2013.

Black, J. T., & Kohser, R. A., "DeGarmo's materials and processes in manufacturing", Journal of Chemical Information and Modeling, Vol. 53(9), 2012.

Box, G., & Draper, N., "Empirical model-building and response surfaces", 1987.

Calamaz, M., Coupard, D., Girot, F., "A new material model for 2D numerical simulation of serrated chip formation when machining titanium alloy Ti–6Al–4V", Vol.48(3-4), PP. 275-288, 2008.

Chandrasekaran, M., & Devarasiddappa, D., "Artificial neural network modeling for surface roughness prediction in cylindrical grinding of Al- SiCp metal matrix composites and ANOVA analysis", Vol.9(2), PP.59-70, 2014.

Chen, X., Rowe, W. B., & Cai, R., "Precision grinding using CBN wheels", International Journal of Machine Tools and Manufacture, Vol.42(5), PP.585–593, 2002.

Chua, M. S., Rahman, M., Wong, Y. S., & Loh, H. T., "Determination of optimal cutting conditions using design of experiments and optimization techniques", International Journal of Machine Tools and Manufacture, Vol.33(2), PP.297-305, 1993.

D., H., & S., M., "Technology environmentaly correct for intern cylindrical grinding", Machines and Metals Magazine, 2001.

da Silva, L. R., Bianchi, E. C., Fusse, R. Y., Catai, R. E., França, T. V., & Aguiar, P. R., "Analysis of surface integrity for minimum quantity lubricant-MQL in grinding", International Journal of Machine Tools and Manufacture, Vol.47(2), PP. 412-418.

Dai, J., Ding, W., Zhang, L., Xu, J., & Su, H., "Understanding the effects of grinding speed and undeformed chip thickness on the chip formation in high-speed grinding", International Journal of Advanced Manufacturing Technology, Vol.81(5–8), PP.995–1005, 2015.

Das, S. K., Choi, S. U. S., Yu, W., & Pradeep, T., "Nanofluids: Science and Technology", Nanofluids: Science and Technology, 2007.

Davim, J., "Machining: fundamentals and recent advances", 2008.

Davim, J. P., Gaitonde, V. N., & Karnik, S. R., "Investigations into the effect of cutting conditions on surface roughness in turning of free machining steel by ANN models", Journal of Materials Processing Technology, Vol.205(1–3), PP.16-23, 2008.

Davis, L. C., & Artz, B. E., "Thermal conductivity of metal-matrix composites", Journal of Applied Physics, Vol.77(10), PP.4954–4960, 1995.

Daymi, A., Boujelbene, M., Ben Salem, S., Hadj Sassi, B., & Torbaty, S., "Effect of the cutting speed on the chip morphology and the cutting forces", Archives of computational materials science and surface engineering, Vol.1(2), PP. 77-83, 2009.

De Mello Belentani, R., Júnior, H. F., Canarim, R. C., Diniz, A. E., Hassui, A., Aguiar, P.

R., & Bianchi, E. C., "Utilization of minimum quantity lubrication (MQL) with water in CBN grinding of steel", Materials Research, Vol.17(1), 2014.

Debnath, S., Reddy, M. M., & Yi, Q. S., "Environmental friendly cutting fluids and cooling techniques in machining: a review", Journal of Cleaner Production, Vol.83, PP.33–47, 2014.

Dhar, N. R., Kamruzzaman, M., & Ahmed, M., "Effect of minimum quantity lubrication (MQL) on tool wear and surface roughness in turning AISI-4340 steel", Journal of Materials Processing Technology, Vol.172(2), PP.299–304, 2006.

Dhar, N., Siddiqui, A.T., Rashid, M. H., "Effect of high pressure coolant jet on grinding temperature, chip and surface roughness in grinding AISI-1040 Steel", ARPN Journal of Engineering and Applied Sciences, Vol.1(4), 2006.

Di Ilio, A., Lambiase, F., & Paoletti, "Grindability assessment of metal matrix composites", Procedia CIRP, Vol.67, PP.313–318, 2018.

Do Nascimento, W. R., Yamamoto, A. A., De Mello, H. J., Canarim, R. C., De Aguiar, P. R., & Bianchi, E. C., "A study on the viability of minimum quantity lubrication with water in grinding of ceramics using a hybrid-bonded diamond wheel", Proceedings of the Institution of Mechanical Engineers, Part B: Journal of Engineering Manufacture, Vol.230(9), 2016.

El-Gallab, M., & Sklad, M., "Machining of Al/SiC particulate metal-matrix composites: Part I: Tool performance", Journal of Materials Processing Technology, Vol.83(1–3), PP.151–158, 1998.

Ghosh, S., "Application of sustainable techniques in metal cutting for enhanced machinability: a review", Vol.100, PP.17-34, 2015.

Groover, M. P., "Fundamentals of Modern Manufacturing: Materials, Processes, and Systems", John Wiley & Sons, 2020.

Guo, Y.B., David W.Y., "A FEM study on mechanisms of discontinuous chip formation in hard machining, Journal of Materials Processing Technology, Vol.155-156, PP. 1350-1356, 2004.

.Hafenbraedl, D., & Malkin, S., "Environmentally-conscious Minimum Quantity

Lubrication (MQL) for Internal Cylindrical Grinding", Transactions of the north american manufacturing research institute of sme, vol. xxviii, 2000.

Hagan, M. T., Demuth, H. B., & Beale, M. H., "Neural Network Design", Boston Massachusetts PWS, Vol. 2, 1995.

Hanrahan, G., Zhu, J., Gibani, S., & Patil, D. G., "chemometrics and statistics | experimental design", Encyclopedia of Analytical Science: Second Edition, PP. 8–13, 2005.

Hosseini, T. A., Shabgard, M., & Pilehvarian, F., "On the feasibility of a reduction in cutting fluid consumption via spray of biodegradable vegetable oil with compressed air in machining Inconel 706", Journal of Cleaner Production, Vol.104, PP.422–435, 2015.

Hung, N. P., Zhong, Z. W., & Zhong, C. H., "Grinding of metal matrix composites reinforced with silicon-carbide particles", Materials and Manufacturing Processes, Vol.12(6), PP.1075–1091, 1997.

Hyung W. P. B., Woodruff, G. W., Liang, S. Y., George W., A. W., Zhou, C. H., Danyluk, S. W., & Griffin, P. H., "Development of micro-grinding mechanics and machine tools", 2008.

Inasaki, I., & Nakayama, K., "High-Efficiency Grinding of Advanced Ceramics", CIRP Annals - Manufacturing Technology, Vol.35(1), PP.211–214, 1986.

Irani, R. A., Bauer, R. J., & Warkentin, A., "A review of cutting fluid application in the grinding process", International Journal of Machine Tools and Manufacture, Vol. 45(15), PP. 1696–1705, 2005.

Jawahir, I.S., van Luttervelt, C.A., "Recent developments in chip control research and applications", CIRP Annals, Vol.42(2), PP. 659-693, 1993.

Kalpakjian, S., & Schmid, S., "Manufacturing engineering and technology", Pearson, 2013.

Kalpana, V. N., Kataru, B. A. S., Sravani, N., Vigneshwari, T., Panneerselvam, A., & Devi Rajeswari, V., "Biosynthesis of zinc oxide nanoparticles using culture filtrates of Aspergillus niger: Antimicrobial textiles and dye degradation studies", OpenNano, Vol.3, PP.48–55, 2018.

Karimi, H., & Yousefi, F., "Application of artificial neural network-genetic algorithm (ANN-GA) to correlation of density in nanofluids", Fluid Phase Equilibria, Vol.336, 2012.

Klocke, F., Soo, S. L., Karpuschewski, B., Webster, J. A., Novovic, D., Elfizy, A., Axinte, D. A., & Tönissen, S., "Abrasive machining of advanced aerospace alloys and composites" CIRP Annals - Manufacturing Technology, Vol.64(2), PP.581–604, 2015.

Kocaefe, M., "Temperature and force modeling on grinding", 2017.

Krabacher, E. J., "Factors Influencing the Performance of Grinding Wheels", Journal of Engineering for Industry,Vol. 81(3), PP.187–199, 1959.

Kuram, E., Ozcelik, B., & Demirbas, E., "Environmentally Friendly Machining: Vegetable Based Cutting Fluids", PP.23–47, 2013.

Kwak, J. S., & Ha, M. K., "Evaluation of wheel life by grinding ratio and static force", KSME International Journal, Vol.16(9), PP.1072–1077, 2002.

Li, S., Wu, Y., & Nomura, M., "Effect of grinding wheel ultrasonic vibration on chip formation in surface grinding of Inconel 718", International Journal of Advanced Manufacturing Technology, Vol.86(1–4), PP.1113–1125, 2016.

Lortz, W., "A model of the cutting mechanism in grinding", Wear, Vol.53(1), PP.115–128, 1979.

Mandal, B., Singh, R., Das, S., & Banerjee, S., "Development of a grinding fluid delivery technique and its performance evaluation", Materials and Manufacturing Processes, Vol.27(4), PP.436–442, 2012.

Mao, C., Tang, X., Zou, H., Zhou, Z., & Yin, W., "Experimental investigation of surface quality for minimum quantity oil-water lubrication grinding", International Journal of Advanced Manufacturing Technology, Vol.59(1–4), 2012.

Mao, C., Zou, H., & Huang, X., "The influence of spraying parameters on grinding performance for nanofluid minimum quantity lubrication", The International Journal of Advanced Manufacturing Technology, Vol.64, PP.1791–1799, 2013.

Merchant, M. E., "Mechanics of the Metal Cutting Process. I. Orthogonal Cutting and a

Type 2 Chip", Journal of Applied Physics, Vol.16(5), PP.267-275, 2004.

Mia, M., & Dhar, N. R., "Prediction of surface roughness in hard turning under high pressure coolant using Artificial Neural Network", Measurement: Journal of the International Measurement Confederation, Vol.92, PP. 464-474, 2016.

Mia, M., & Dhar, N. R., "Influence of single and dual cryogenic jets on machinability characteristics in turning of Ti-6Al-4V", Proceedings of the Institution of Mechanical Engineers, Part B: Journal of Engineering Manufacture, Vol.233(3), 2019.

Mohan, A. C., & Renjanadevi, B., "Preparation of zinc oxide nanoparticles and its characterization using scanning electron microscopy (SEM) and x-ray diffraction(XRD)", Procedia Technology, Vol.24, PP.761–766, 2016.

Nandakumar, A., & Rajmohan, T., "Grinding of MMC using MQL based vegetable oil - Review", IOP Conference Series: Materials Science and Engineering, Vol.390(1), 2018.

Nas, E., & Gökkaya, H., "Experimental and statistical study on machinability of the composite materials with metal matrix Al/B4C/Graphite", Metallurgical and Materials Transactions, Vol. 48(10), PP.5059–5067, 2017.

Okumus, S. C., Aslan, S., Karslioglu, R., Gultekin, D., & Akbulut, H., "Thermal expansion and thermal conductivity behaviors of al-si/sic/graphite hybrid metal matrix composites (MMCs)", Materials Science ,Vol. 18(4), PP. 341–346, 2012.

Rahman, M. M., & Kadirgama, K., "Performance of water-based zinc oxide nanoparticle coolant during abrasive grinding of ductile cast iron", 2014.

Raj, D. A., & Senthilvelan, T., "Empirical modelling and optimization of process parameters of machining titanium alloy by Wire-EDM using RSM", Materials Today: Proceedings, Vol.2(4–5), 2015.

Rowe, W. B., "Principles of modern grinding technology", 2013.

Rowe, W. B., Black, S. C. E., Mills, B., Morgan, M. N., & Qi, H. S., "Grinding temperatures and energy partitioning", Proceedings of the Royal Society A: Mathematical, Physical and Engineering Sciences, Vol.453(1960), PP.1083–1104, 1997.

Rowe, W. B., Morgan, M. N., Batako, A., & Jin, T., "Energy and temperature analysis in grinding", Laser Metrology and Machine Performance, Vol. VI, 2003.

Sadeghi, M. H., Haddad, M. J., Tawakoli, T., & Emami, M., "Minimal quantity lubrication-MQL in grinding of Ti-6Al-4V titanium alloy", International Journal of Advanced Manufacturing Technology,Vol. 44(5–6), PP.487–500, 2009.

Sadhukhan, B., Mondal, N. K., & Chattoraj, S., "Optimisation using central composite design (CCD) and the desirability function for sorption of methylene blue from aqueous solution onto Lemna major", Karbala International Journal of Modern Science, Vol.2(3), PP.145–155, 2016.

Said, Z., Gupta, M., Hegab, H., Arora, N., Khan, A. M., Jamil, M., & Bellos, E., "A comprehensive review on minimum quantity lubrication (MQL) in machining processes using nano-cutting fluids", International Journal of Advanced Manufacturing Technology, Vol.105(5–6), PP.2057–2086, 2019.

Sarabia, L. A., & Ortiz, M. C., "Response Surface Methodology", Comprehensive Chemometrics, Vol.1, PP.345–390, 2009.

Setti, D., Sinha, M.K., Ghosh, S., Rao, P. V., "Performance evaluation of Ti–6Al–4V grinding using chip formation and coefficient of friction under the influence of nanofluids", International Journal of Machine Tools and Manufacture, Vol.88, PP. 237-248, 2015.

Shanawaz, A. M., Sundaram, S., Pillai, U. T. S., & Babu Aurtherson, P., "Grinding of aluminium silicon carbide metal matrix composite materials by electrolytic in-process dressing grinding", International Journal of Advanced Manufacturing Technology, Vol.57(1–4), PP.143–150, 2011.

Shen, B., Shih, A. J., & Tung, S. C., "Application of nanofluids in minimum quantity lubrication grinding", Tribology Transactions, Vol.51(6), 2008.

Shokoohi, Y., & Shekarian, E., "Application of nanofluids in machining processes-a review", Journal of Nanoscience and Technology, Vol.59-63. 2015.

Silva, L. R., Bianchi, E. C., Catai, R. E., Fusse, R. Y., França, T. V., & Aguiar, P. R., "Study on the behavior of the Minimum quantity lubricant - MQL technique under different lubricating and cooling conditions when grinding ABNT 4340 steel",

Journal of the Brazilian Society of Mechanical Sciences and Engineering, Vol.27(2), 2005.

Sima, M., & Ozel, T., "Modified material constitutive models for serrated chip formation simulations and experimental validation in machining of titanium alloy Ti–6Al–4V", International Journal of Machine Tools and Manufacture, Vol.50(11), PP. 943-960, 2010.

Sinha, M. K., Madarkar, R., Ghosh, S., & Rao, P. V., "Application of eco-friendly nanofluids during grinding of Inconel 718 through small quantity lubrication", Journal of Cleaner Production, Vol.141, PP.1359–1375, 2017.

SUS Choi, J. E., "Enhancing thermal conductivity of fluids with nanoparticles, developments and applications of non-newtonian flows", ASME, Vol.38, 1995.

Svozil, D., Kvasnička, V., & Pospíchal, J., "Introduction to multi-layer feed-forward neural networks", Chemometrics and Intelligent Laboratory Systems, Vol.39(1), 1997.

Tawakoli, T., Hadad, M. J., & Sadeghi, M. H., "Influence of oil mist parameters on minimum quantity lubrication - MQL grinding process", International Journal of Machine Tools and Manufacture, Vol.50(6), PP.521–531, 2010.

Teicher, U., Künanz, K., Ghosh, A., & Chattopadhyay, A. B., "Performance of diamond and CBN single-layered grinding wheels in grinding titanium", Materials and Manufacturing Processes, Vol.23(3), PP.224–227, 2008.

Tolouei-Rad, M., & Bidhendi, I. M., "On the optimization of machining parameters for milling operations", International Journal of Machine Tools and Manufacture, Vol.37(1), PP.1–16, 1997.

Tso, P. L., "An investigation of chip types in grinding", Journal of Materials Processing Tech., Vol.53(3–4), PP.521–532, 1995.

Tusar, M. I. H., Zaman, P. B., Mia, M., Saha, S., & Dhar, N. R., "Influence of grinding parameters on surface roughness and temperature under carbon nanotube assisted MQL", PP.1–24, 2022.

Wang, J., "Multiple-objective optimisation of machining operations based on neural

networks", The International Journal of Advanced Manufacturing Technology, Vol.8(4), 1993.

Yasa, E., Pilatin, S., & Çolak, O., "Overview of cryogenic cooling in machining of Ti alloys and a case study", Journal of Production Engineering, Vol. 15(2), PP.1-9, 2012.

Zain, A. M., Haron, H., & Sharif, S., "Prediction of surface roughness in the end milling machining using Artificial Neural Network", Expert Systems with Applications, Vol.37(2), 2010.

Zaman, P. B., Tusar, M. I. H., & Dhar, N. R., "Selection of appropriate process inputs for turning Ti-6Al-4V alloy under hybrid Al2O3-MWCNT nano-fluid based MQL", Advances in Materials and Processing Technologies, Vol.8(1), PP. 380-400, 2020.

Zhong, Z., & Hung, N. P., "Diamond turning and grinding of aluminum-based metal matrix composites", Materials and Manufacturing Processes, Vol.15(6), PP.853–865, 2000.

Zhong, Z., & Hung, N. P., "Grinding of alumina/aluminum composites", Journal of Materials Processing Technology, Vol.123(1), PP.13–17, 2002.